

SKB

**TECHNICAL
REPORT**

87-27

**Earthquake measurements in southern
Sweden**

Oct 1, 1986 – Mar 31, 1987

Ragnar Slunga
Leif Nordgren

Swedish Defence Research Establishment
Department 2
Stockholm

December 1987

SVENSK KÄRNBRÄNSLEHANTERING AB

SWEDISH NUCLEAR FUEL AND WASTE MANAGEMENT CO

BOX 5864 S-102 48 STOCKHOLM

TEL 08-665 28 00 TELEX 13108-SKB

EARTHQUAKE MEASUREMENTS IN SOUTHERN SWEDEN
OCT 1, 1986 - MAR 31, 1987

Ragnar Slunga, Leif Nordgren

Försvarets Forskningsanstalt, Huvudavdelning 2
Stockholm December 1987

This report concerns a study which was conducted for SKB. The conclusions and viewpoints presented in the report are those of the author(s) and do not necessarily coincide with those of the client.

Information on KBS technical reports from 1977-1978 (TR 121), 1979 (TR 79-28), 1980 (TR 80-26), 1981 (TR 81-17), 1982 (TR 82-28), 1983 (TR 83-77), 1984 (TR 85-01), 1985 (TR 85-20) and 1986 (TR 86-31) is available through SKB.

SUMMARY

A network of four stations covering southeastern Sweden has been operated for the period Oct 1 1986 - Mar 31 1987. The project is financed by SKB. During the period no earthquakes within the four station network were detected. Seven other earthquakes in southern Sweden were detected and they have been analysed by use of data from all seismic stations operated by Foa. Three of these events were aftershocks to the strong Skoevde event, 860714, ML=4.5. This made it necessary to include the Skoevde main event together with a couple of earlier aftershocks in the analysis presented in this report. Thus the present study gives 10 new earthquake mechanisms. Three of these events are in the range ML=3.5-4.5. Of the earlier about 170 earthquake mechanisms available for southern Sweden the largest is ML=3.2. The earthquakes of the present study thus give significant new information about Swedish seismic activity. The results are:

- the focal depths of the larger events of the lake Vaernern area are about 27 km, this is deeper than the most common earthquake depths 7-18 km, actually all but one of the earthquakes in this report are deeper than 18 km
- the horizontal stresses relaxed by the new earthquakes agree with previous studies, WNW-ESE compression
- the static stress drops are high for the larger events, above 30 MPa (300 bar) for the ML=4.5 event
- the Skoevde main shock fault is striking ENE, this is different from the N-S striking fault shown to be sliding during the lake Vaernern event 810213, ML=3.2
- the aftershocks to the Skoevde events migrate upwards with a rate of about 10 km per year
- the large events seem to occur in small gaps within the microseismicity of the previous 5 years
- the faulting mechanisms are primarily strike-slip at rather vertical faults.

CONTENT

Summary	4
Content	5
Introduction	6
The data acquisition and event detection methods	7
The earthquakes	8
The relation to the previous seismicity	10
The geographical distribution	11
The focal depths	13
Vertical migration of the stress release	15
The Skoevde event and its aftershocks	17
The horizontal stresses	22
The seismic moments, static stress drops, fault radii, and fault slips	24
Discussion and conclusions	26
References	28
Appendix 1. The earthquake source parameters and fault plane solutions	29

INTRODUCTION

SKB (Swedish nuclear fuel and waste management Co) finances a seismic network in southeastern Sweden. The network has been established and is operated by Foa (National defence research institute) in Stockholm. In addition to the four stations included in the SKB network for this period, 861001-870331, data from four more stations in central and western Sweden were available in the analysis. These other stations have been operated for the purpose of monitoring the global seismicity. Figure 1 shows the locations of the stations from which data have been available.

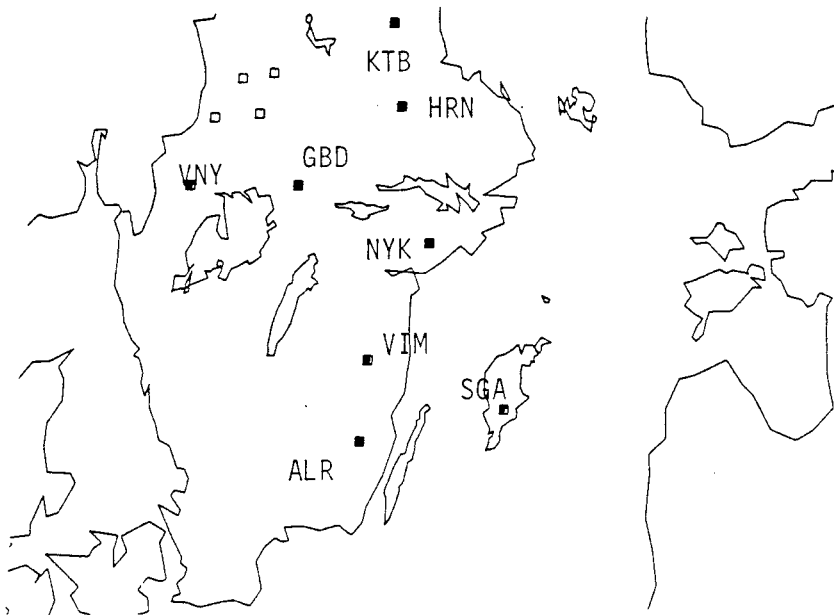


Figure 1. The stations VIM, ALR, SGA, and NYK defines the area of main interest to the present study. Data from the Hagfors Observatory (open squares) and from the stations KTB, HRN, GBD, and VNY have also been available.

This report covers the period 861001-870331. During this period no earthquakes within the area of primary interest were recorded. However, the data allow also studies of larger events outside this area. The results of the analysis of 7 such events are presented in this report. Three of these events turned out to be aftershocks to the Skoevde event 860714 1350GMT, ML=4.5. This required also the main event to be analysed together with two of its aftershocks. Thus source mechanism results of totally 10 events are given in this report.

THE DATA ACQUISITION AND EVENT DETECTION METHODS

All stations transmit continuously frequency modulated signals to the central computer at Foa in Stockholm. Permanent telephone lines are used. Gain ranging amplifiers prohibit overloading. The signals and gain information are sampled at a rate of 60 Hz. At Stockholm the analogue signals are bandpass filtered (5-15Hz) and fed into a S/N-detector. When three or four close stations give detections within a time window corresponding to the seismic travel time between the stations an event detection is declared and the data is saved on digital tape. At least one minute of data before the detections are included. In this way about 20-40 detected "events" per day are stored on tape. This means that the continuous data flow has been reduced by a factor 0.1-0.15.

The magnetic tapes are then copied into the disc-memory, demultiplexed and submitted to an automatic analysis. The output of this analysis is a list of located seismic events which are given together with plots of the signals. The list and plot are then checked by the seismologist. Most of the regular mining explosions are in this way automatically located and identified and there is normally no need for further interactive analysis of most of the events. As almost all local events are explosions this means a great reduction of the time consuming interactive analysis.

In the interactive analysis the seismologist decides what to save for further source mechanism studies. This means that automatic algorithms for fault plane solution, size determination and if needed relative location are run.

The methods for fault plane solution, for estimation of the dynamic source parameters, and for relative location are described by Slunga (1981, 1982).

The data for the period (861001-870331) is contained on 400 magnetic standard tapes.

The availability of the data acquisition system for the period was 97%, the loss was due to regular service and to tape station problems. Thus the data covers 97% of the total time.

THE EARTHQUAKES

The earthquakes analysed in this report are listed in table 1 together with the origin times, locations, depths, and magnitudes. The three events prior to Oct 1986 are included because three of the events within the period Oct 1986 - Mar 1987 are aftershocks to that sequence.

Table 1. The earthquakes analysed in this report.

Date	Origin time UNT	Epicenter lat N long E		Focal depth (km)	Seismic moment (Nm)	ML	Direction horizontal compression deg N to E
860714	135036.0	58.432	13.996	26.6	0.73E+15	4.5	126.
860714	144532.2	58.433	13.995	25.2	0.51E+14	3.6	106.
860714	152836.2	58.417	13.969	24.9	0.11E+13	2.0	153.
861102	0748 0.7	58.770	13.730	26.7	0.38E+14	3.5	115.
870107	193742.9	58.435	13.935	21.9	0.12E+13	2.1	155.
870129	100210.5	58.433	13.975	(18.0)	0.24E+12	1.4	
870202	094654.5	61.157	16.652	20.6	0.10E+13	2.0	46.
870218	155258.6	60.070	12.525	20.2	0.71E+12	1.9	118.
870317	023734.2	60.156	15.858	5.3	0.53E+12	1.7	99.
870320	204211.7	58.426	13.978	19.3	0.98E+12	2.0	114.

Figure 2 shows their geographical distribution together with the locations of the previously analysed events.

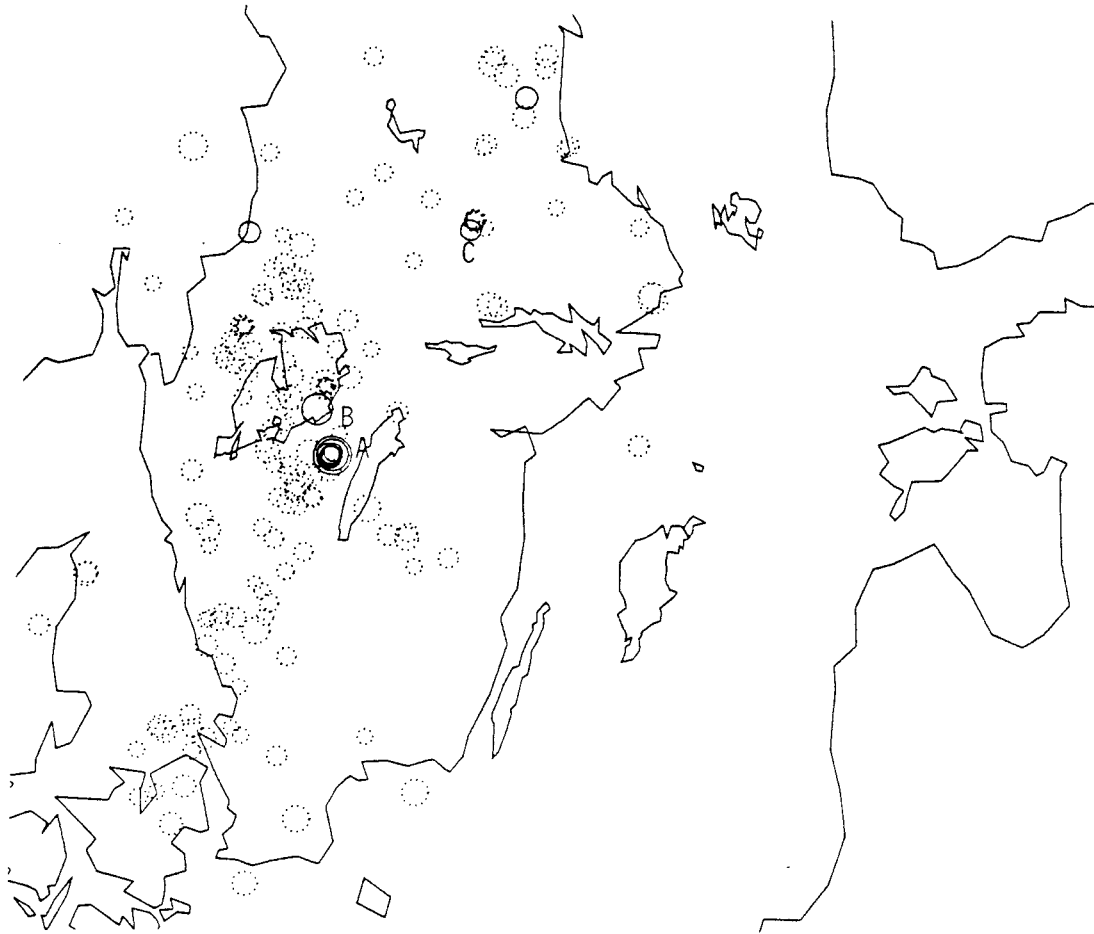


Figure 2. The earthquakes that are included in this report are given by the solid circles. The dotted circles show the previously analysed earthquakes of the period 1979-1985. All these earthquakes have been analysed in the same way. The letter A marks the Skoevde events, B marks the ML=3.5 lake Vaenern event 861102, C marks the only event of this report having a focal depth less than 18km (depth is 5km). This event is close to the shallow swarm of 1981.

The detailed results for each earthquake are given in appendix 1.

THE RELATION TO THE PREVIOUS SEISMICITY

During the years 1979-1984, covered by the earthquake research project at Foa financed by SKI, detailed source information and fault plane solutions from some 150 earthquakes in southern Sweden were achieved, Slunga, Norrman and Glans (1984) and Slunga (1985). The largest event recorded during that period had magnitude $M_L=3.2$. During the period 1985-1986 three M_L 4-4.5 earthquakes in addition to three M_L 3.5-3.6 occurred. This means a large change in the activity, no such serial of large events has occurred since the 1904 major earthquake, $M_s=5.5$, and the following years. Unfortunately the SKI decided not to continue the study in spite of the very interesting geophysical results achieved. Most of the seismic stations in western Sweden were closed and no earthquake monitoring of south-western Sweden comparable to the Foa network has since then been done. This means that we do not have knowledge about the microseismicity for the years 1985-1987, see figure 3. The present project started at Oct 1 1986 but does not have a coverage for south-western Sweden comparable to the earlier coverage. However, the comparison of the larger later events with the earlier microseismicity shows several interesting features.

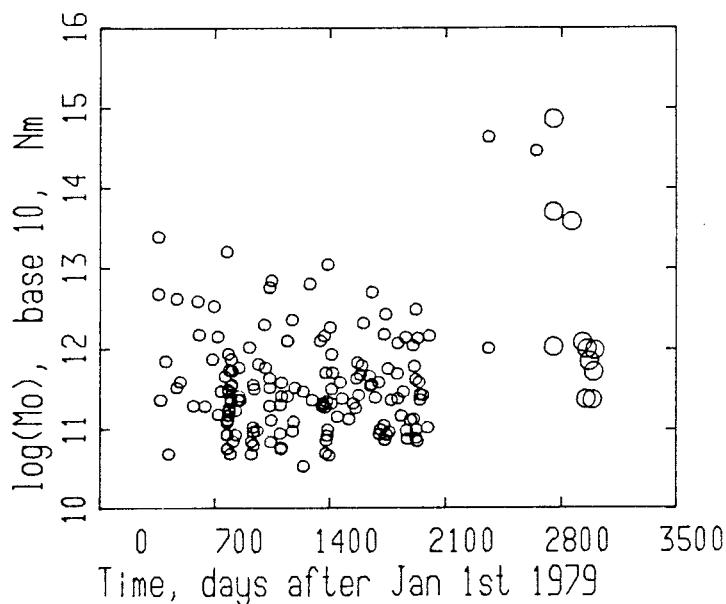


Figure 3. The time distribution of the earlier seismicity, small circles, and of the earthquakes analysed in this report, larger circles. Unfortunately we do not have coverage of the microseismicity for the whole time interval.

THE GEOGRAPHICAL DISTRIBUTION

In figure 2 the locations of the earthquakes included in the present analysis are shown. Although the events occurred in the active areas they have a clear tendency to fill gaps. This is more clear in figure 4 showing the lake Vänern area.



Figure 4. The location of the two large earthquakes analysed in this report (solid circles) in relation to the previous microseismicity (dotted circles). The sizes of the circles reflects the magnitudes. The aftershocks to the Skoevde event are also included. It is obvious that the solid circles are located in gaps of the previous microseismicity.

It is clear from figure 2 that the earthquakes are not distributed uniformly. In order to get some quantification of the distances involved figure 5 was prepared. It shows the distribution of distances between events. All distances between all events were computed and the frequencies were divided by the expected frequencies for a uniform

distribution. This ratio was called the "relative frequency ratio" and is plotted in figure 5 for the events in south-western Sweden during 1980-1984. Only distances up to 100 km are included in the figure and the uniform distribution was normalized to give the same total number of inter-event distances as the real observations.

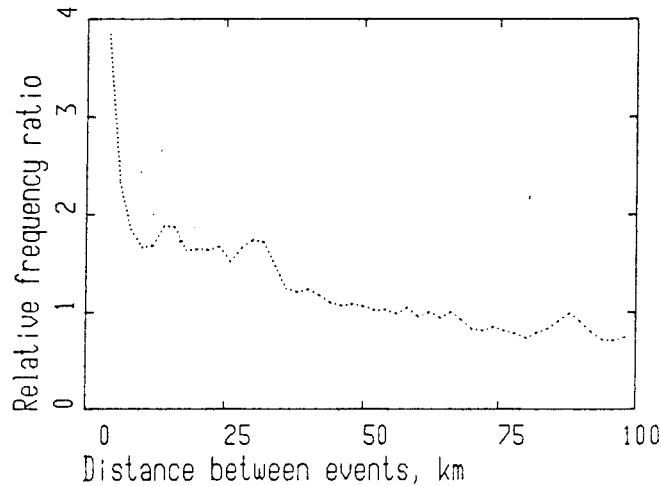


Figure 5. The diagram shows the frequency of inter-event distances. All distances between all events in the western part of southern Sweden have been computed for the events during the period 1980-1984. The frequencies have then been divided by the frequencies expected for a uniform epicenter distribution. The density of the uniform distribution has been adjusted to the observations in the distance interval 0-100 km. If our observed inter-event distances belonged to a uniform distribution the ratio would be constant and equal to 1 in the figure. This is obviously not the case for these events.

The distribution shown in figure 5 has following features:

- the number of very closely spaced events is high up to some 10 km
- in the distance range 10-35 km there seems to be a uniform distribution almost twice as dense as in the whole distance range 0-100 km
- in the range 35-100 km the frequency ratio falls from 1.2 to 0.7, that means a slight deviation from uniform distribution.

The conclusion is that there is a tendency to geographical clustering, especially within distances up to 35 km. This distance has the same size as the thickness of the seismogenic layer, the deepest earthquakes occur at 30-35 km depth, (for one exception see Slunga (1985)).

THE FOCAL DEPTHS

As can be seen in table 1 the focal depths of both the Skoevde events and the ML=3.5 lake Vaernern event are about 25 km. This is fairly large. In figure 6 the focal depths and seismic moments are plotted.

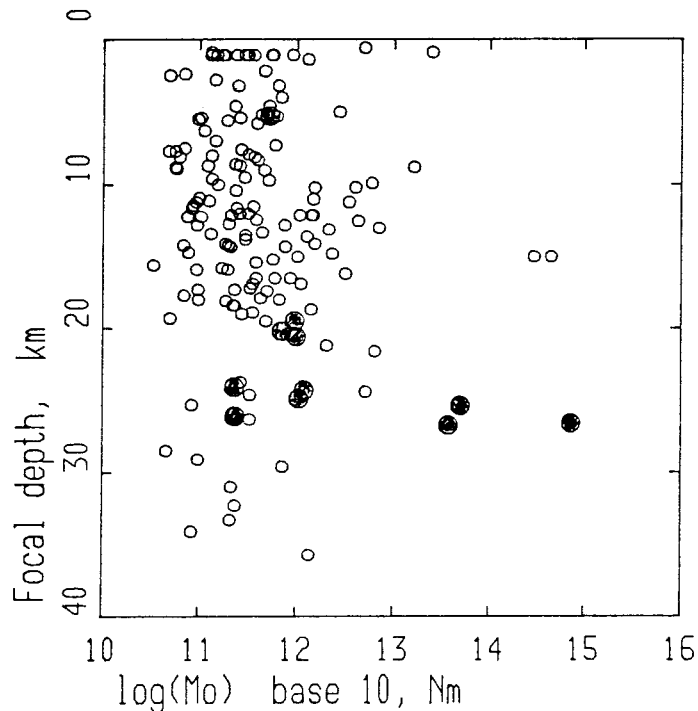


Figure 6. The focal depths and seismic moments. The previous seismicity is marked by small circles, the presently studied earthquakes by filled large circles. Notice that all but one event are below the most frequent depth interval, 7-19km.

Slunga, Norrman, and Glans (1984) pointed out that the earthquakes below and above 20km depth apparently were different populations with different b-values. A larger portion large earthquakes occurs at greater depths. This is also indicated by the present investigation.

The two large events at about 12-15 km depth in figure 6 are the Kattegatt events close to the Tornquist line having fault plane solutions fitting that strike. It is interesting to notice that these events (ML 4.1-4.5) occur at the depth of most Swedish earthquakes 8-18 km, contrary to the Skoevde events that belong to the deeper population. In this context one should also mention the strong earthquake in the Gulf of Finland 1976, ML=5, which occurred at 12 km

depth, Slunga (1979).

In figure 7 geographical and depth distribution of the lake Vaernern area is shown. Most of the previous seismicity is much more shallow and it seems evident that the two larger deep events are in gaps within the area of preceding microseismicity.

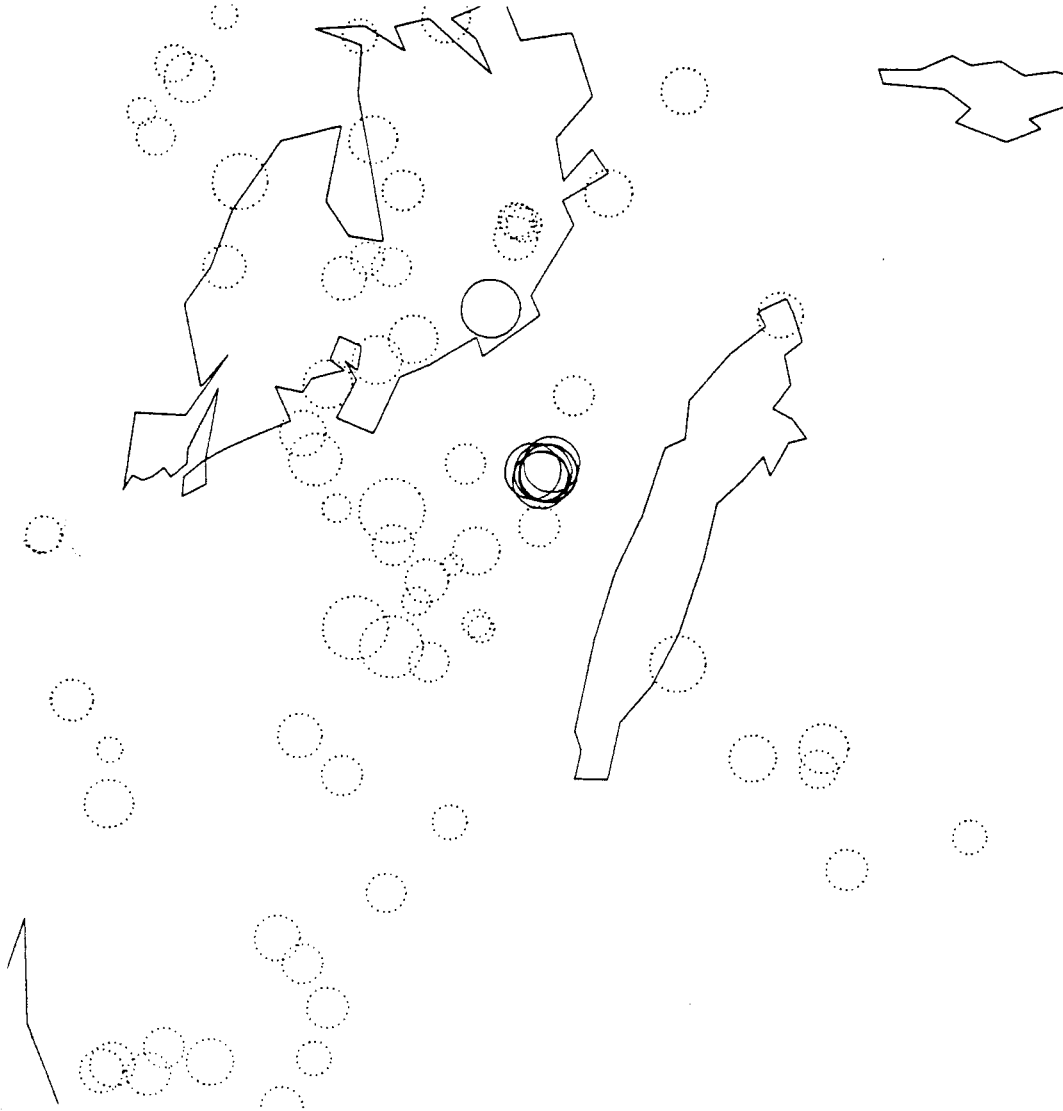


Figure 7. The epicenters of the earthquakes in the lake Vaernern area. The size of the circles are proportional to the focal depths. The solid circles belong to events of table 1.

In conclusion the recent large events of the lake Vaernern area have occurred at larger depths than most events during the previous six years, and at gaps in the seismicity within the active parts.

VERTICAL MIGRATION OF THE STRESS RELEASE

One interesting aspect of the Skoevde earthquakes is the vertical migration. The later events (during Jan-Mar 1987) are at about 4-8 km more shallow depths. This means a vertical migration upwards at a rate of 8-16 km per year.

It is obvious that the tectonic stresses can be expected to migrate upwards from the softer deep crust where the stresses are released by ductile deformations. The clear picture of the Skoevde activity supports this view.

There have been other deep earthquakes within some 50 km from the Skoevde events. In order to check the idea of vertical migration I plotted the picture given in figure 8. It shows the focal depths and times of the earthquakes in the area surrounding the Skoevde activity.

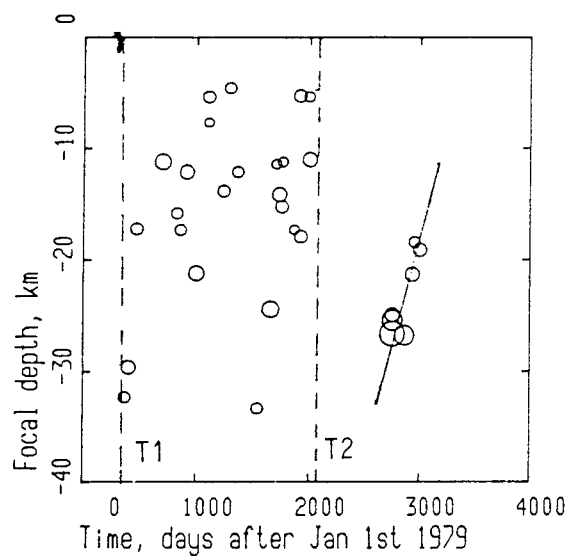


Figure 8. The horizontal axis gives the origin times and the vertical axis gives the focal depths of the earthquakes in the area 13-15 deg east, 58-59 deg north. The time T1 and T2 mark the starting time and the stopping time of the monitoring of the microseismicity. The late events to the right are the events presented in this report. The straight line through the Skoevde events shows roughly the rate of vertical migration for those events.

The idea of presenting figure 8 is to point out that it may be possible to detect stress migrations by use of the micro-seismicity. Although one cannot draw conclusions from figure 8 it is obvious that there may be a vertical migration component in the activity. The deep events seem to be followed by activity successively higher up in the crust up to some 5 km depth. If there really is a general vertical stress release migration it may however be a very complex 3D phenomena. Essential parts of the process may be aseismic which means that a complete picture cannot be achieved by seismic studies, other geophysical methods must probably be included. It would for instance be interesting to have geodetic monitoring or tilt measurements of the active areas. Such measurements may detect aseismic faulting.

THE SKOEVEDE EVENT AND ITS AFTERSHOCKS

As mentioned above the focal depths are less for the later aftershocks showing a vertical migration of the stress release.

The fault plane solutions are summarized in figure 9 for these events.

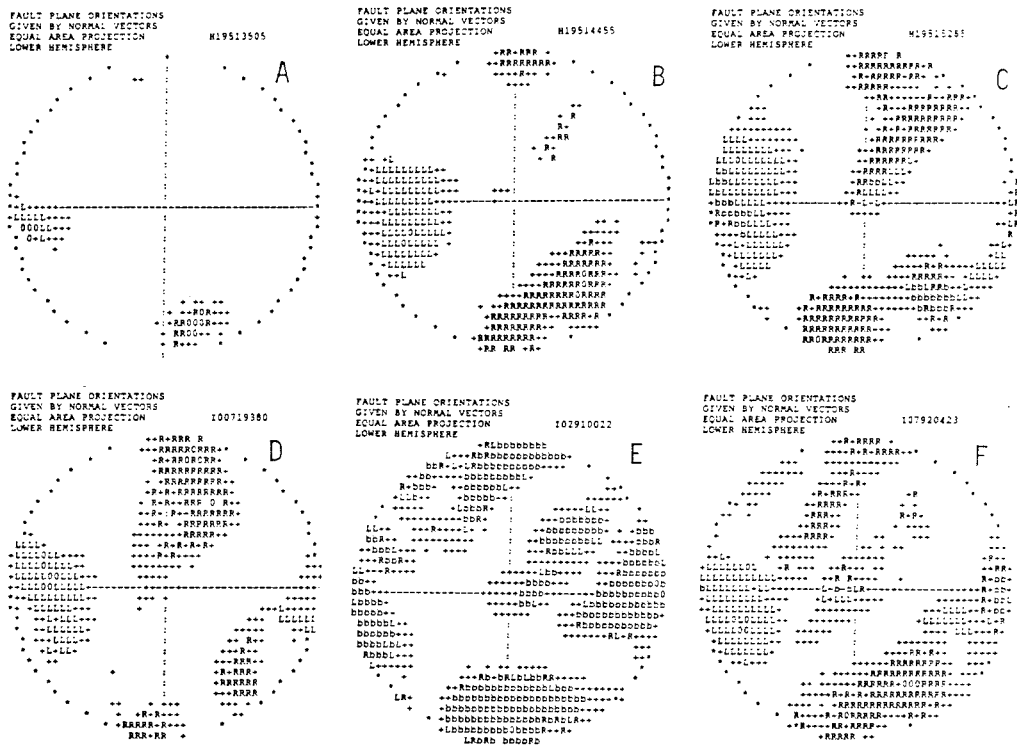


Figure 9. The fault plane solutions for the Skoevde events. Each circle pertains to one event and gives the range of acceptable fault plane orientations. The fault planes are given by the directions of the fault plane normals in equal area projections of the lower hemisphere. A marks the main shock. The very best fitting orientations are marked by O, while the letters R and L mark acceptable orientations with right or left lateral movements, b marks acceptable planes with both directions of movements.

The events A, B, and C occurred at the same day and at about the same focal depth, 26 km. The events D and F have focal depths about 20 km, the depth of E is more uncertain but probably similar to D and F. The events D and E occurred in Jan 87, half a year after the main shock, event F occurred in March 87.

For the main shock a rather unique fault plane solution is achieved. Due to the nonuniqueness of the low frequency fault plane inversion two possible plane orientations are given as is clearly seen for event A. The best fitting planes of event A are contained in the group of acceptable orientations for events B, E, and F. The best fitting planes of events B, E, and F are however rotated about 15-20 degrees compared to the main shock. The events C and D do not contain the best fitting planes of event A among the acceptable fault planes. The optimum planes of events C and D are rotated some 30 degrees compared to the best fitting planes of event A.

One interpretation of the fault plane solutions is that the events occur on a system of fractures close to each other but with 15-30 degrees differences in orientation, the fault slips are in rather similar directions.

In order to discriminate the two possible fault planes given by the fault plane solution the algorithm developed at Foa for relative location (Slunga (1982) and Slunga, Norrman, and Glans (1984)) was applied. Figure 10 gives the results of the relative location by means of the directions of the normals to the planes that best fitted the resulting locations of the three events of Jul 14 1986, events A, B, and C. The results are also given in table 2.

Table 2. Relative locations of the main shock and the two aftershocks at the same day. The location of the main shock, A, is reference. The estimated standard deviations of the relative locations are about 60m.

Date	GMT	ML(Mo)	East	North	Z (up)	Fault radius	
860714	1350	A	4.5	0m	0m	130-220m	
860714	1445	B	3.6	347	28	36	100-180
860714	1528	C	2.0	124	115	160	60-100

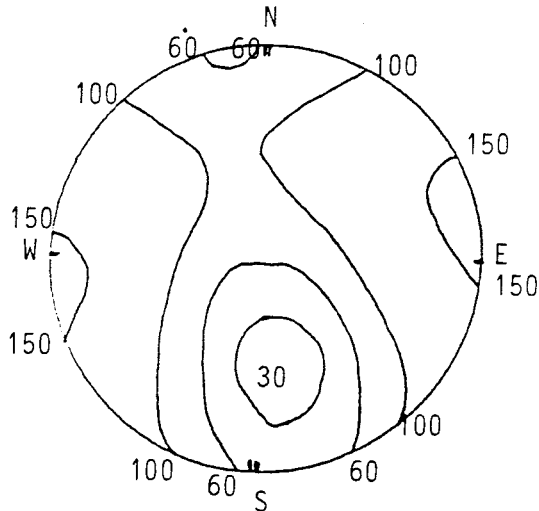


Figure 10. The results of the relative location of events A, B, and C are given by use of an equal area projection of the lower hemisphere for showing plane normal directions. The numbers at the lines give the RMS value of the deviations of the relative locations from the plane. We see that planes having normals dipping 35 deg in SSE direction best fit the relative location. From the estimates of the uncertainties of the relative locations we take RMS values up to 60 m as acceptable.

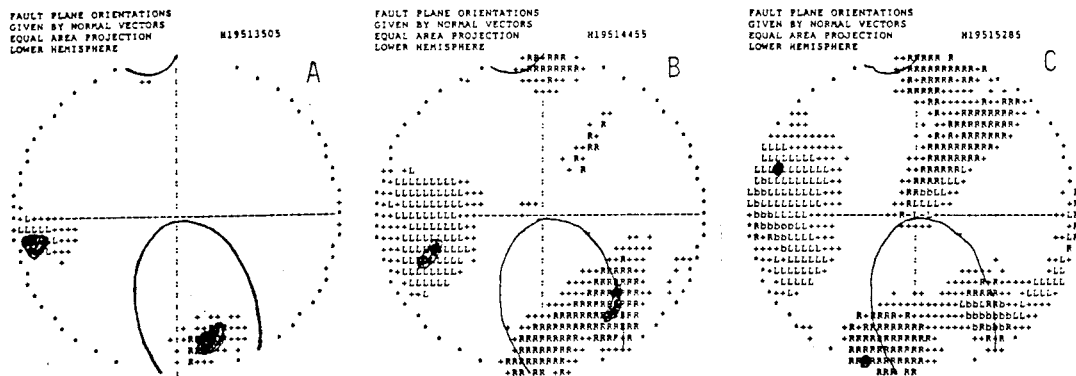


Figure 11. Comparison between the result of the relative location of A, B, and C and their fault plane solutions. The 60 m contour of figure 10 is used. The fair agreement is a strong indication that the ENE-WSW fault plane possibility dipping north is the true fault plane.

The results of the relative location fits rather well one of

the possibilities given by the fault plane solutions, the ENE-WSW striking, north dipping plane.

The fault plane solutions of the later aftershocks are also very similar to the first day's events although the depths are several kilometers smaller. This indicates that they probably occurs on the same system of ENE-striking faults.

The result that it is not the more N-S striking fault plane possibility that is likely to be the true one is a little surprising. The well-established fault plane of the lake Vaern event Feb 13 1981, Slunga, Norrman, and Glans (1984), has the strike N-S (N10W). However the lake Vaern event 1981 had a focal depth of some 9 km while the Skoevde main event occurred at some 26 km depth. In discussions with prof Pedersen at Uppsala University he mentioned that ENE-oriented deeper crustal faults in this area are indicated by recent electrical investigations.

The in plane positions are shown in figure 12 together with the upper limits of the fault radii. It can be seen that the B event is outside the estimated fault area of the main event, A, while the C event is to a larger extent within the faulting surfaces of events A and B.

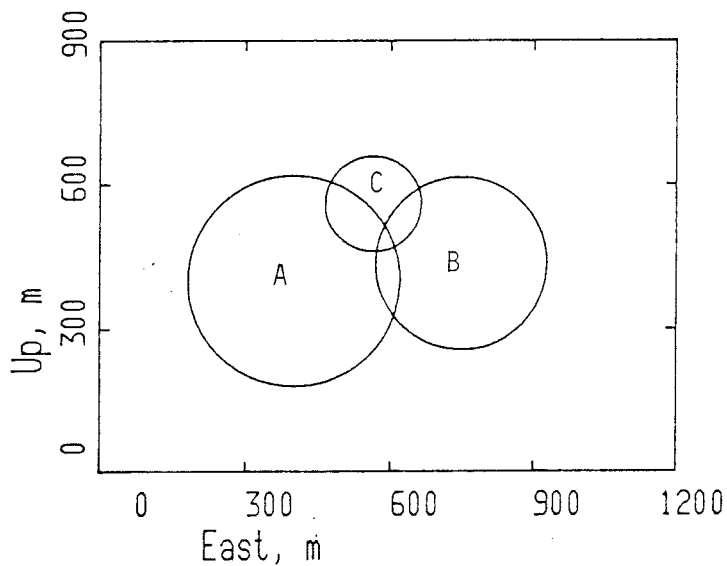


Figure 12. The relative positions of the three events in the fault plane. The radii of the circles are the upper bounds of the fault radii ranges as estimated from the corner frequencies.

In the study of the 810213 event (ML=3.2) and its aftershocks Slunga et al (1984) found that the aftershocks occurred within the estimated fault surface. Also the greatest after-

shock was 2.1 magnitude (ML) units smaller and had a stress drop about $1/30$ of that of the main shock. In this case the strong aftershock B is only 0.9 magnitudes less and the stress drop is $1/3$ of that of the main shock, A. This supports the result of the relative location and of the fault radius estimation that the second shock is not a stress relaxation at the original fault surface but a twin event extending the faulting surface. Actually the fault plane solution indicates that it might be on a fault deviating some 15-20 degrees from the main fault. The third event, C, has a stress drop of only $1/60$ of the main shock which is in agreement with the stress relaxation theory. It also occurred to a larger extent within the faulting surfaces of the previous events. One can also notice that the third event is above the central part of the total faulting surface of the two previous events. This is very similar to the lake Vaenern aftershocks mentioned above.

THE HORIZONTAL STRESSES

One of the early important results of the Foa research on the Nordic seismic activity was the determination of the orientation of the regional horizontal stresses. In figure 13 the stresses relaxed by the present events are shown together with the earlier results from Slunga, Norrman, and Glans (1984).



Figure 13. The orientation and relative size of the horizontal deviatoric stresses relaxed by the earthquake slips. The solid lines are the earthquakes of this study, the dashed lines are taken from Slunga, Norrman, and Glans (1984). Only the very best fitting fault plane solution is shown for each event, often several fault plane solutions are almost equally good.

The stresses relaxed by the events presented in this report

are in good agreement with the earlier results. The forces driving the earthquake slips have the same horizontal direction.

THE SEISMIC MOMENTS, STATIC STRESS DROPS, FAULT RADII,
AND FAULT SLIPS

The seismic moments focal depths and ranges of static stress drops and fault slips are given in table 3. The values of these parameters are computed from the estimated corner frequencies. This is discussed by Slunga et al (1984).

Table 3. The dynamic source parameters: seismic moment, static stress drop, peak slip at the fault, and fault radius. The letters marks events of the Skoevde group.

Date	GMT	Depth km	Moment Nm	Stress drop MPa	Peak fault slip mm	Fault radius m
860714	1350	A 26	0.74E+15	30-140	160-470	130-220
860714	1445	B 25	0.51E+14	4- 20	20- 50	100-180
860714	1528	C 25	0.11E+13	0.5-2.4	1.2-3.5	60-100
861102	0748	27	0.38E+14	10- 40	30- 80	70-120
870107	1938	D 22	0.12E+13	.08-.26	0.4-0.8	130-190
870129	1002	E (18)	0.24E+12	.03-.17	0.1-0.4	80-140
870202	0946	21	0.10E+13	0.7- 2	1.5- 3	30- 90
870218	1552	20	0.71E+12	0.4-1.6	0.9-1.4	60-100
870317	0237	5	0.53E+12	0.2-1.4	0.6-1.2	50-110
870320	2042	F 19	0.98E+12	.13-.39	0.5-1.1	100-150

It is interesting to note the very high static stress drops of the three earthquakes having seismic moments larger than $1E+13$ Nm ($M_L > 3$). The focal depths are about 26 km.

In figure 14 the static stress drops and seismic moments are related to the previous seismicity as given by Slunga et al (1984).

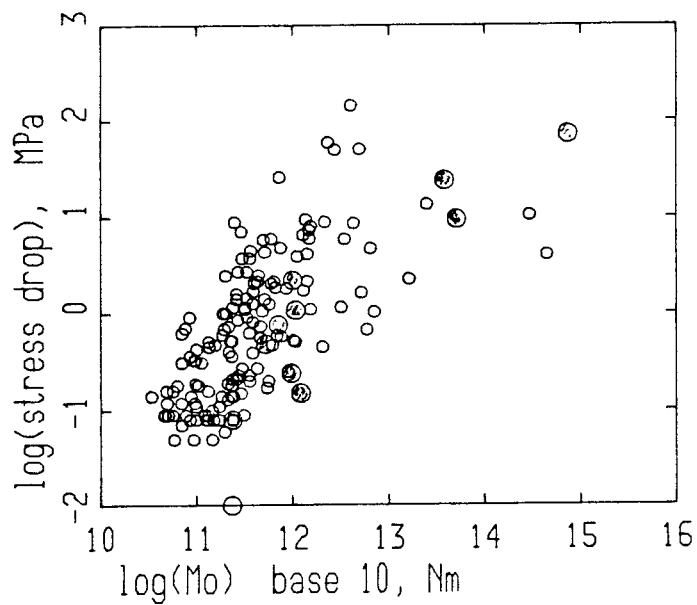


Figure 14. The static stress drop as function of the seismic moment. The filled large circles are the earthquakes of the present study, the smaller circles mark earthquakes from the years 1980-1985.

In relating the Swedish seismic activity to geological and tectonic processes it is also interesting to note the large peak slips involved, about 200 mm or more for the main event at Skoevde.

DISCUSSION AND CONCLUSIONS

Of the ten earthquakes analysed in this report all but one have focal depths deeper than 18 km, that means below the most frequent earthquake depths. This indicates that the seismicity of the last two years represents another stage or phase than the preceding seismicity.

The direction of the relaxed horizontal stresses, WNW-ESE orientated compression, is in perfect agreement with the earlier studies.

The aftershocks to the Skoevde event shows a migration upwards at a rate of about 10 km per year based on data from half a year.

One possibility to the differences in focal depths may be that the activity of the last years represent a phase in the vertical migration of stress and/or stress release. It is also worth noting that the $ML > 4$ events in Kattegatt, 850615 and 860401, at focal depths of about 13 km, preceded this activity. Although these events are much too small to affect directly what happens up in the lake Vaern area the closeness in time and space between the Kattegatt activity ($ML=4.4$ and 4.1), the Skoevde events ($ML=4.5$ and 3.6), and the lake Vaern event ($ML=3.6$) is an indication that a common tectonical episodic event may lie behind. For instance one can think of significant aseismic slip at some fault system followed by horizontal stress migration or ductile deformations in the lower parts of the lithosphere leading to vertical stress migration up to the seismogenic upper crust.

The high static stress drops for the three largest events in this report is interesting. This is probably related to the great focal depths, about 26 km. Greater shear stresses can be expected due to the greater compressive stresses at such depths. The earlier noticed tendency for larger events to have larger stress drops is also verified by the new events. A stress drop above 30 MPa (300 bar) as estimated for the Skoevde main event is however higher than the standard values often assumed for even large intraplate earthquakes. The Kattegatt event ($ML=4.4$ and focal depth 13 km) had lower static stress drop: 1.3-8 MPa. Slunga (1982) noticed however already that the Scania events (NW-SE faults with normal faulting components like the Kattegatt events) had smaller static stress drop estimates than other Swedish earthquakes.

The analysis of the Skoevde main event and aftershocks indicates that the faulting may have occurred on a system of closely spaced faults with various strikes in the range ENE plus/minus 25 degrees.

The relative location of the Skoevde events indicates that the fault radii computed from the corner frequency estimates may be on the small side. One must however keep in mind that one assumption in the interpretation of the corner frequencies is that the faulting area is circular. If the area is elongated the corner frequency analysis may give the smaller dimension.

REFERENCES

Båth, M. (1956). An earthquake catalogue for Fennoscandia for the years 1891-1950. Sveriges Geologiska Undersökning, Avhandlingar och uppsatser, C 545, Stockholm.

Båth, M. (1979). Earthquakes in Sweden 1951-1976. Sveriges Geologiska Undersökning, Avhandlingar och uppsatser, C 750, Uppsala.

Hasegawa, H.S., Adams, J. och Yamazaki, K. (1985). Upper crustal stresses and vertical stress migration in eastern Canada. Journ. Geophys. Res., 90, pp. 3637-3648.

Slunga, R.S. (1979). Source mechanism of a Baltic earthquake inferred from surface wave recordings, Bull. Seism. Soc. Am., 69, pp. 1931-1964.

Slunga, R.S. (1981a). Earthquake source mechanism determination by use of body-wave amplitudes - an application to Swedish earthquakes. Bull. Seism. Soc. Am., 71, pp. 25-35.

Slunga, R.S. (1981b). Fault mechanisms of Fennoscandian earthquakes and regional crustal stresses. Geol. Föreningens i Stockholm Förhandlingar, 103, pp. 27-31.

Slunga, R.S. (1982). Research on Swedish earthquakes 1980-1981. FOA Report C 20477-T1.

Slunga, R.S., Norrman, P. and Glans A.-C. (1984a). Seismicity of southern Sweden. FOA Report C 20543-T1.

Slunga, R.S., Norrman, P. and Glans A.-C. (1984b). Baltic shield seismicity, the results of a regional network. Geophys. Res. Letters, 11, pp. 1247-1250.

Slunga, R.S. (1985). The seismicity of southern Sweden, 1979-1984, final report. Foa report C 20572-T1, April 1985, ISSN 0347-3694, Stockholm.

APPENDIX 1

THE EARTHQUAKE SOURCE PARAMETERS AND FAULT PLANE SOLUTIONS

The source parameters of the following earthquakes are given:

Date	Origin time UNT	Epicenter lat N long E		Focal depth (km)	ML	
860714	135036.0	58.432	13.996	26.6	4.5	Skoevde main shock
860714	144532.2	58.433	13.995	25.2	3.6	" aftershock
860714	152836.2	58.417	13.969	24.9	2.0	" "
861102	0748 0.7	58.770	13.730	26.7	3.5	Lake Vaenern
870107	193742.9	58.435	13.935	21.9	2.1	Skoevde aftershock
870129	100210.5	58.433	13.975	(18.0)	1.4	" "
870202	094654.5	61.157	16.652	20.6	2.0	SV Soederhamn
870218	155258.6	60.070	12.525	20.2	1.9	Vermland
870317	023734.2	60.156	15.858	5.3	1.7	Bergslagen
870320	204211.7	58.426	13.978	19.3	2.0	Skoevde aftershock

For each event the following are given:

The arrival time observations and the results of the location algorithm.

The input data to the fault plane inversion, first motion directions and spectral amplitudes for vertical P and S.

The output of the fault plane inversion algorithm: the dynamic source parameters, the very best fitting fault mechanism, and statistical information.

Plots showing all acceptable orientations of the P- and T-axes and of the fault plane normals. These are given in equal area projections of the lower hemisphere. A fourth circular diagram gives all acceptable relative horizontal deviatoric stresses. This plot of the horizontal deviatoric stress is symmetric around the center of the circle, each point marked in the circle is an endpoint of a line going through the center to corresponding symmetrical point. The lines marked by the endpoints gives the orientation and relative size of the horizontal deviatoric stresses for acceptable solutions. The relative size is 1 for a diameter (strike slip on a vertical fault). The orientation of the line gives the orientation of the principal horizontal compression, the principal horizontal tension is normal to the line.

The marks in the plots of the P- and T-axes and of the

horizontal deviatoric stresses have the following meaning:

- + less well fitting mechanism
- O well fitting mechanism
- 0 optimum mechanisms.

The marks in the plot of the fault plane normals mean:

- + less well fitting mechanism
- R well fitting right-lateral plane
- L well fitting left-lateral plane
- b well fitting plane both right- and left-lateral
- 0 best fitting planes.

860714 135036.0 58.432 13.996 26.6 4.5 Skoevde main shock

ORIGIN TIME 86 07 14 13H 50M 36.0S +/- 0.18S ***
 LATITUDE 58.432 +/- 0.014 DEG. 13.km from n:o 11
 LONGITUDE 13.996 +/- 0.031 Billingen EM.
 FOCAL DEPTH 26.6 +/- 2.6 KM ***

STA	ARR.	TIME	RES.	WEIGHT	DIST.	AZIMUTH	
GBD	P	13 50 55.21	0.19	23.4	118.7	15.5	P UP
GBD	S	13 51 8.87	-0.41	0.3	118.7	15.5	
VIM	P	13 50 57.76	-0.20	19.8	138.5	120.4	P DOWN
VNY	P	13 50 58.03	-0.04	19.7	139.2	321.8	P DOWN
VNY	S	13 51 14.94	0.29	0.3	139.2	321.8	
NYK	P	13 51 4.60	-0.09	6.1	187.9	71.7	
HFS	P	13 51 4.49	-0.53	6.0	190.6	355.0	P DOWN
ALR	P	13 51 6.50	0.68	5.8	197.1	143.6	
HRN	P	13 51 12.38	0.36	1.9	247.4	33.9	
HRN	S	13 51 39.70	0.47	0.0	247.4	33.9	
SGA	P	13 51 17.98	0.19	1.5	294.2	113.4	P DOWN
KTB	P	13 51 20.31	-0.76	1.3	320.7	22.7	P UP

INPUT DATA FOR FAULT PLANE SOLUTION

STN	DIST.	AZIMUTH	OMEGA(PZ)	OMEGA(SZ)
	KM	DEGREES	METER-SEC	METER-SEC
GBD	119.	15.3	+ 0.56E-06	+ 0.25E-05
VIM	138.	120.4	- 0.41E-06	0.71E-06
VNY	140.	321.8	- 0.76E-06	0.17E-05
NYK	188.	71.6	0.25E-06	0.40E-05
SGA	294.	113.4	- 0.00E+00	0.00E+00
KTB	321.	22.6	+ 0.00E+00	0.00E+00
HFS	191.	354.9	- 0.00E+00	0.00E+00

DYNAMIC SOURCE PARAMETERS

SIZE MEASURES

SEISMIC MOMENT: 0.735E+15 Nm

LOCAL MAGNITUDE: 4.5

SHEAR WAVE CORNER FREQUENCY RANGE AT CLOSE DISTANCES (150km)
 3.1Hz - 5.3Hz (4.2Hz)

FAULT RADIUS RANGE 130m - 222m (164m)

STRESS DROP RANGE 29.17MPa -145.79MPa (72.55MPa)

RANGE OF THE PEAK SLIP AT THE FAULT 163.0mm -476.6mm (299.3mm)

860714 135036.0 58.432 13.996 26.6 4.5 Skoevde main shock
FOR THE BEST FITTING MECHANISM

THE ORIENTATION OF THE RELAXED STRESS

	AZIMUTH	DIP
P-AXIS	124.	5. degrees
T-AXIS	36.	-22.

THE HORIZONTAL DEVIATORIC STRESS AS GIVEN BY THE P- AND T-AXES
THE AZIMUTH OF COMPRESSION -54 degrees
THE RELATIVE SIZE 0.92

THE TWO POSSIBLE FAULT PLANES

	STRIKE	DIP	SLIP
PLANE A	78.	71.	-12. degrees
PLANE B	172.	78.	200.

THE NORMAL DIRECTIONS OF THE FAULT PLANES

	AZIMUTH	DIP
PLANE A	168.	19. degrees
PLANE B	262.	12.

STRIKE SLIP FAULTING DOMINATES

STATISTICAL INFORMATION

OF 7 FIRST MOTION POLARITY OBSERVATIONS
AT LEAST 7 ARE REQUIRED TO FIT

THE OPTIMUM MECHANISM HAS 0 POLARITY MISFITS

AMPLITUDES FOR P AND S AT 4 STATIONS ARE USED
ONLY MECHANISMS GIVING AN ESTIMATED STANDARD
DEVIATION OF THE AMPLITUDE ERROR FACTOR OF LESS
THAN 2.00 FOR SINGLE P-WAVE OBSERVATIONS ARE
TAKEN AS ACCEPTABLE AND INCLUDED IN THE FIGURES

0.41 % OF ALL MECHANISMS ARE ACCEPTABLE
2.1 % ACCEPTABLE DUE TO FIRST MOTION OBSERVATIONS
19.6 % OF THESE FITTED ALSO THE AMPLITUDES
THE PART OF WELL FITTING PLANES IS 2.4%

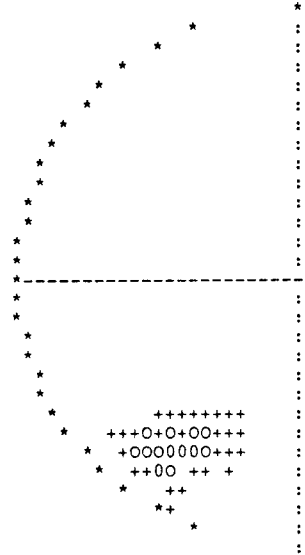
THE AMPLITUDE FIT OF THE OPTIMAL MECHANISM
GIVES A MEAN ERROR FACTOR OF 1.44
THIS CORRESPONDS TO A STANDARD DEVIATION FACTOR OF 1.68
FOR SINGLE P-WAVE OBSERVATIONS

THE DOUBLE COUPLE SOLUTION IS SIGNIFICANT
AT 35 % LEVEL
(F-VALUE: $F(7, 4) = 1.57$)

860714 135036.0 58.432 13.996 26.6 4.5 Skoevde main shock

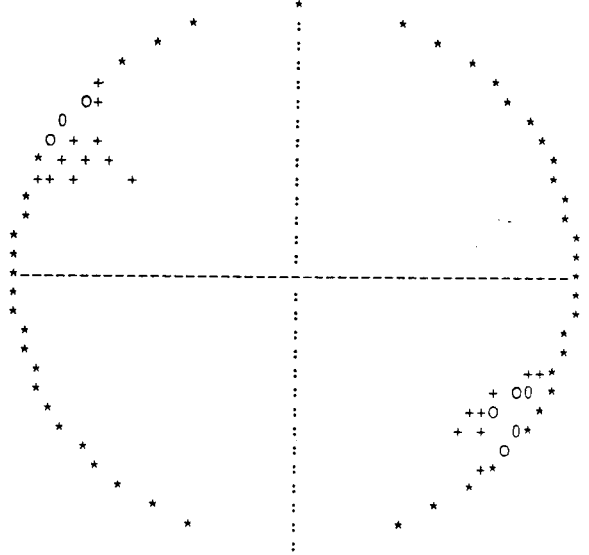
T-AXIS ORIENTATIONS
EQUAL AREA PROJECTION
LOWER HEMISPHERE

H19513505



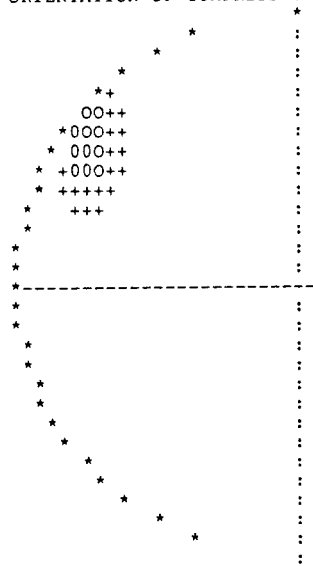
P-AXIS ORIENTATIONS
EQUAL AREA PROJECTION
LOWER HEMISPHERE

H19513505



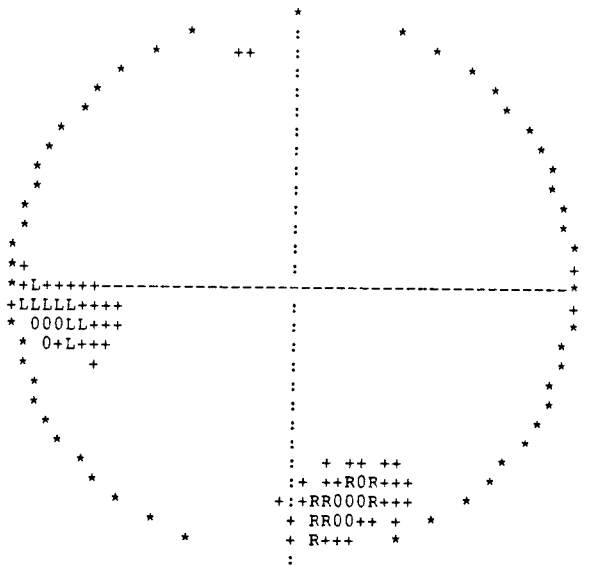
HORIZONTAL DEVIATORIC STRESS
RELATIVE SIZE AND
ORIENTATION OF COMPRESSION

H19513505



FAULT PLANE ORIENTATIONS
GIVEN BY NORMAL VECTORS
EQUAL AREA PROJECTION
LOWER HEMISPHERE

H19513505



860714 144532.2 58.433 13.995 25.2 3.6 Skoevde aftershock

ORIGIN TIME 86 07 14 14H 45M 32.2S +/- 0.18S ***
 LATITUDE 58.433 +/- 0.014 DEG. 13.km from n:o 11
 LONGITUDE 13.995 +/- 0.031 Billingen EM.
 FOCAL DEPTH 25.4 +/- 2.6 KM ***

STA	ARR.	TIME	RES.	WEIGHT	DIST.	AZIMUTH	
GBD	P	14 45 51.40	0.21	23.4	118.7	15.5	P UP
GBD	S	14 46 5.04	-0.39	0.3	118.7	15.5	
VIM	P	14 45 53.92	-0.23	19.8	138.6	120.4	P DOWN
VIM	S	14 46 11.62	0.96	0.3	138.6	120.4	
VNY	P	14 45 54.19	-0.04	19.7	139.1	321.8	P DOWN
VNY	S	14 46 11.07	0.29	0.3	139.1	321.8	
NYK	P	14 46 0.89	-0.09	6.1	188.0	71.7	
NYK	S	14 46 22.78	-0.05	0.1	188.0	71.7	
HFS	P	14 46 0.76	-0.54	6.0	190.5	355.0	
ALR	P	14 46 2.87	0.75	5.8	197.2	143.6	
HRN	P	14 46 8.55	0.23	1.9	247.4	33.9	
HRN	S	14 46 35.68	0.08	0.0	247.4	33.9	
SGA	P	14 46 14.27	0.17	1.5	294.3	113.4	
KTB	P	14 46 16.59	-0.76	1.3	320.7	22.7	

INPUT DATA FOR FAULT PLANE SOLUTION

STN	DIST.	AZIMUTH	OMEGA(PZ)	OMEGA(SZ)
	KM	DEGREES	METER-SEC	METER-SEC
GBD	118.	15.5	+ 0.23E-07	+ 0.28E-06
VNY	139.	321.5	- 0.41E-07	0.83E-07
VIM	139.	120.8	- 0.18E-07	0.63E-07
NYK	187.	71.9	0.27E-07	0.12E-06
HRN	247.	34.0	0.87E-08	0.73E-07
SGA	294.	113.6	0.20E-07	0.50E-07

DYNAMIC SOURCE PARAMETERS

SIZE MEASURES

SEISMIC MOMENT: 0.509E+14 Nm

LOCAL MAGNITUDE: 3.6

SHEAR WAVE CORNER FREQUENCY RANGE AT CLOSE DISTANCES (150km)
 3.9Hz - 6.6Hz (5.2Hz)

FAULT RADIUS RANGE 104m - 176m (132m)

STRESS DROP RANGE 4.02MPa - 19.50MPa (9.54MPa)

RANGE OF THE PEAK SLIP AT THE FAULT 17.9mm - 51.2mm (31.8mm)

860714 144532.2 58.433 13.995 25.2 3.6 Skoevde aftershock
FOR THE BEST FITTING MECHANISM

THE ORIENTATION OF THE RELAXED STRESS

	AZIMUTH	DIP
P-AXIS	107.	-1. degrees
T-AXIS	196.	43.

THE HORIZONTAL DEVIATORIC STRESS AS GIVEN BY THE P- AND T-AXES
THE AZIMUTH OF COMPRESSION -74 degrees
THE RELATIVE SIZE 0.77

THE TWO POSSIBLE FAULT PLANES

	STRIKE	DIP	SLIP
PLANE A	-20.	119.	147. degrees
PLANE B	233.	118.	34.

THE NORMAL DIRECTIONS OF THE FAULT PLANES

	AZIMUTH	DIP
PLANE A	250.	29. degrees
PLANE B	143.	28.

STRIKE SLIP FAULTING DOMINATES

STATISTICAL INFORMATION

OF 4 FIRST MOTION POLARITY OBSERVATIONS
AT LEAST 4 ARE REQUIRED TO FIT

THE OPTIMUM MECHANISM HAS 0 POLARITY MISFITS

AMPLITUDES FOR P AND S AT 6 STATIONS ARE USED
ONLY MECHANISMS GIVING AN ESTIMATED STANDARD
DEVIATION OF THE AMPLITUDE ERROR FACTOR OF LESS
THAN 2.00 FOR SINGLE P-WAVE OBSERVATIONS ARE
TAKEN AS ACCEPTABLE AND INCLUDED IN THE FIGURES

3.50 % OF ALL MECHANISMS ARE ACCEPTABLE
10.4 % ACCEPTABLE DUE TO FIRST MOTION OBSERVATIONS
33.6 % OF THESE FITTED ALSO THE AMPLITUDES
THE PART OF WELL FITTING PLANES IS 18.3%

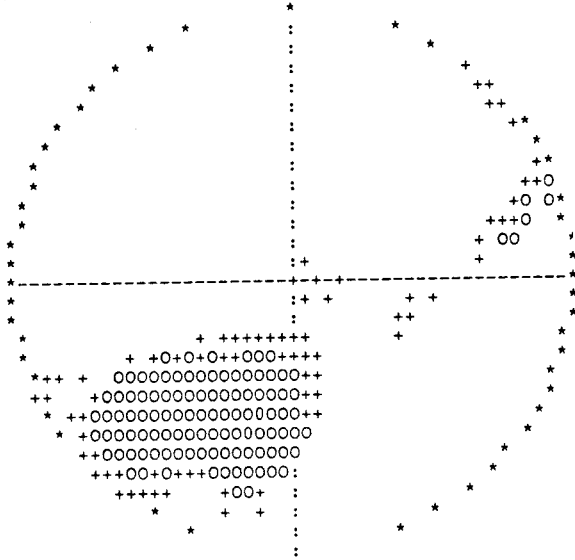
THE AMPLITUDE FIT OF THE OPTIMAL MECHANISM
GIVES A MEAN ERROR FACTOR OF 1.35
THIS CORRESPONDS TO A STANDARD DEVIATION FACTOR OF 1.44
FOR SINGLE P-WAVE OBSERVATIONS

THE DOUBLE COUPLE SOLUTION IS SIGNIFICANT
AT 10 % LEVEL
(F-VALUE: $F(11, 8) = 2.50$)

860714 144532.2 58.433 13.995 25.2 3.6 Skoevd aftershock

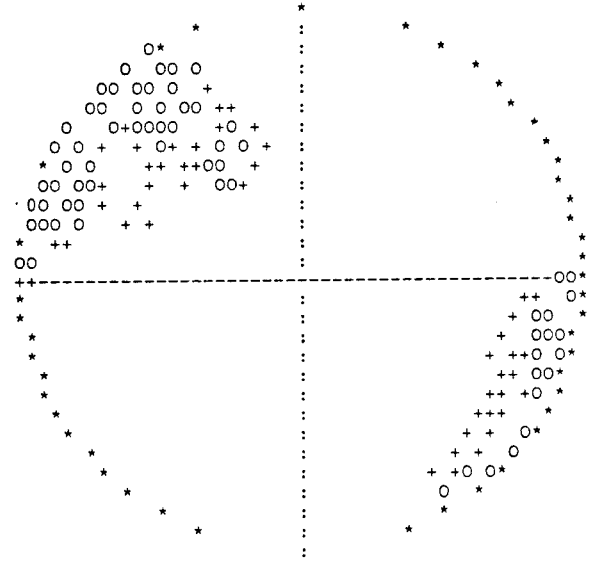
T-AXIS ORIENTATIONS
EQUAL AREA PROJECTION
LOWER HEMISPHERE

H19514455



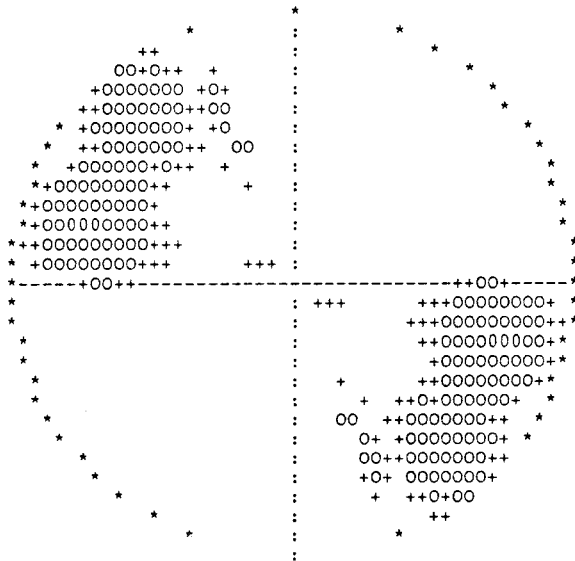
P-AXIS ORIENTATIONS
EQUAL AREA PROJECTION
LOWER HEMISPHERE

H19514455



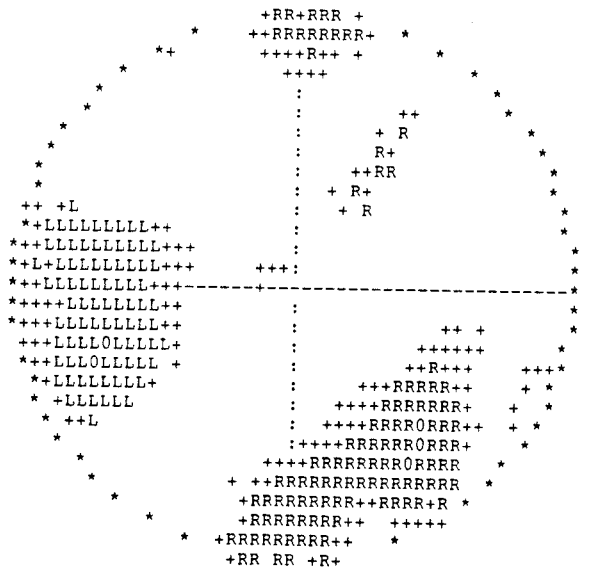
HORIZONTAL DEVIATORIC STRESS
RELATIVE SIZE AND
ORIENTATION OF COMPRESSION

H19514455



FAULT PLANE ORIENTATIONS
GIVEN BY NORMAL VECTORS
EQUAL AREA PROJECTION
LOWER HEMISPHERE

H19514455



860714 152836.2 58.417 13.969 24.9 2.0 Skoevde aftershock

ORIGIN TIME 86 07 14 15H 28M 36.2S +/- 0.21S ***
 LATITUDE 58.417 +/- 0.017 DEG. 11.km from n:o 11
 LONGITUDE 13.969 +/- 0.034 Billingen EM.
 FOCAL DEPTH 24.9 +/- 4.7 KM ***

STA	ARR.	TIME	RES.	WEIGHT	DIST.	AZIMUTH	
GBD	P	15 28 55.47	0.02	23.0	120.8	16.0	
GBD	S	15 29 9.00	-0.92	0.3	120.8	16.0	
VIM	P	15 28 58.16	-0.01	19.7	139.0	119.5	
VNY	P	15 28 58.23	-0.01	19.7	139.5	322.7	P DOWN
VNY	S	15 29 14.80	-0.05	0.3	139.5	322.7	
NYK	P	15 29 5.25	0.02	6.1	190.0	71.4	
NYK	S	15 29 26.40	-0.90	0.1	190.0	71.4	

INPUT DATA FOR FAULT PLANE SOLUTION

STN	DIST.	AZIMUTH	OMEGA(PZ)	OMEGA(SZ)
	KM	DEGREES	METER-SEC	METER-SEC
GBD	120.	16.0	0.43E-09	+ 0.20E-08
VIM	139.	119.6	0.52E-09	0.15E-08
VNY	139.	322.6	- 0.95E-09	0.28E-08
NYK	190.	71.4	0.87E-09	0.33E-08
HRN	249.	34.0	0.26E-09	0.14E-08

DYNAMIC SOURCE PARAMETERS

SIZE MEASURES

SEISMIC MOMENT: 0.108E+13 Nm
 LOCAL MAGNITUDE: 2.0

SHEAR WAVE CORNER FREQUENCY RANGE AT CLOSE DISTANCES (150km)
 7.0Hz -11.8Hz (9.1Hz)

FAULT RADIUS RANGE 58m - 98m (75m)

STRESS DROP RANGE 0.49MPa - 2.35MPa (1.08MPa)

RANGE OF THE PEAK SLIP AT THE FAULT 1.2mm - 3.5mm (2.1mm)

860714 152836.2 58.417 13.969 24.9 2.0 Skoevde aftershock
FOR THE BEST FITTING MECHANISM

THE ORIENTATION OF THE RELAXED STRESS

	AZIMUTH	DIP
P-AXIS	153.	-6. degrees
T-AXIS	62.	-13.

THE HORIZONTAL DEVIATORIC STRESS AS GIVEN BY THE P- AND T-AXES
THE AZIMUTH OF COMPRESSION -27 degrees
THE RELATIVE SIZE 0.97

THE TWO POSSIBLE FAULT PLANES

	STRIKE	DIP	SLIP
PLANE A	107.	86.	-14. degrees
PLANE B	198.	76.	185.

THE NORMAL DIRECTIONS OF THE FAULT PLANES

	AZIMUTH	DIP
PLANE A	197.	4. degrees
PLANE B	288.	14.

STRIKE SLIP FAULTING DOMINATES

STATISTICAL INFORMATION

OF 2 FIRST MOTION POLARITY OBSERVATIONS
AT LEAST 2 ARE REQUIRED TO FIT

THE OPTIMUM MECHANISM HAS 0 POLARITY MISFITS

AMPLITUDES FOR P AND S AT 5 STATIONS ARE USED
ONLY MECHANISMS GIVING AN ESTIMATED STANDARD
DEVIATION OF THE AMPLITUDE ERROR FACTOR OF LESS
THAN 2.00 FOR SINGLE P-WAVE OBSERVATIONS ARE
TAKEN AS ACCEPTABLE AND INCLUDED IN THE FIGURES

6.26 % OF ALL MECHANISMS ARE ACCEPTABLE
24.7 % ACCEPTABLE DUE TO FIRST MOTION OBSERVATIONS
25.4 % OF THESE FITTED ALSO THE AMPLITUDES
THE PART OF WELL FITTING PLANES IS 28.7%

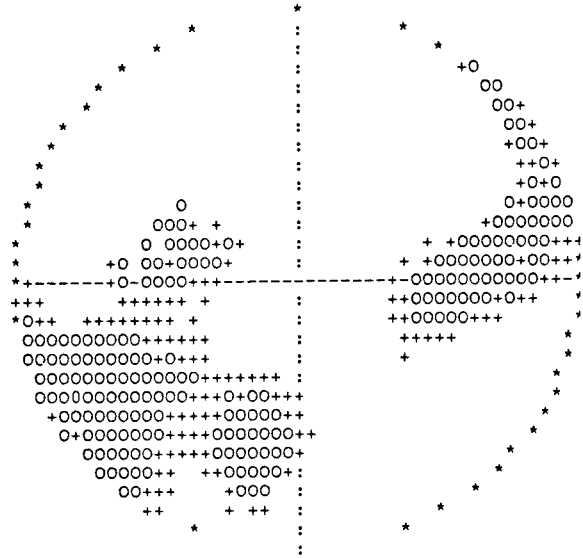
THE AMPLITUDE FIT OF THE OPTIMAL MECHANISM
GIVES A MEAN ERROR FACTOR OF 1.20
THIS CORRESPONDS TO A STANDARD DEVIATION FACTOR OF 1.26
FOR SINGLE P-WAVE OBSERVATIONS

THE DOUBLE COUPLE SOLUTION IS SIGNIFICANT
AT 3 % LEVEL
(F-VALUE: $F(9, 6) = 4.65$)

860714 152836.2 58.417 13.969 24.9 2.0 Skoevde aftershock

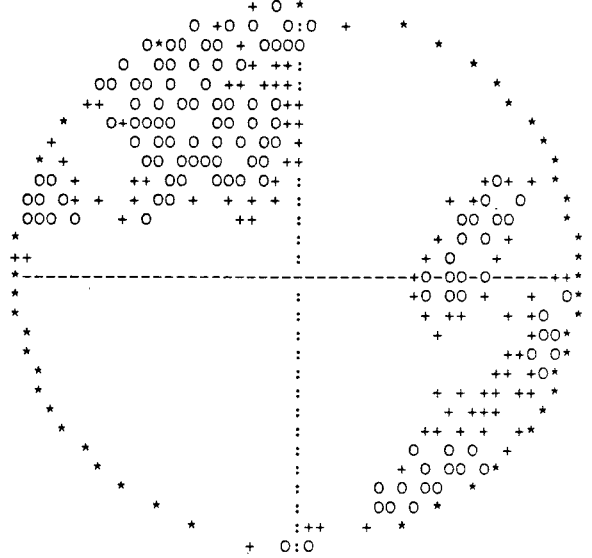
T-AXIS ORIENTATIONS
EQUAL AREA PROJECTION
LOWER HEMISPHERE

H19515285



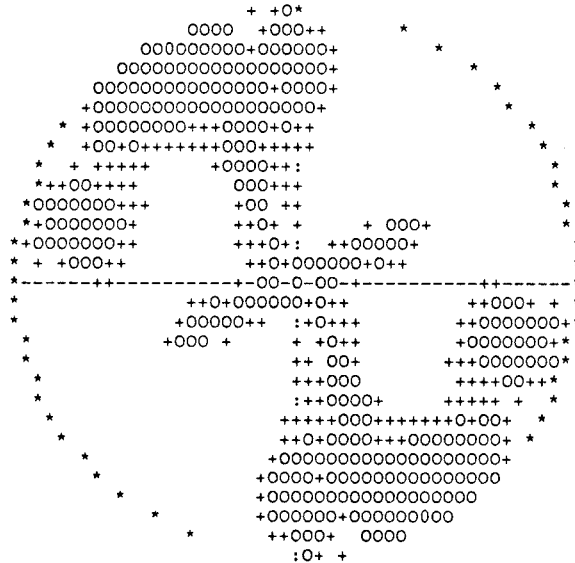
P-AXIS ORIENTATIONS
EQUAL AREA PROJECTION
LOWER HEMISPHERE

H19515285



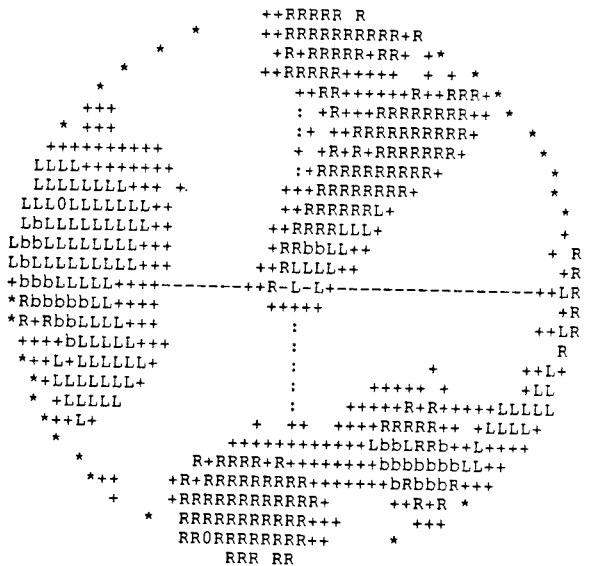
HORIZONTAL DEVIATORIC STRESS
RELATIVE SIZE AND
ORIENTATION OF COMPRESSION

H19515285



FAULT PLANE ORIENTATIONS
GIVEN BY NORMAL VECTORS
EQUAL AREA PROJECTION
LOWER HEMISPHERE

H19515285



861102 0748 0.7 58.770 13.730 26.7 3.5 Lake Vaernern

ORIGIN TIME 86 11 02 07H 48M 0.7S +/- 0.27S ***
 LATITUDE 58.770 +/- 0.021 DEG. 30.km from n:o 99
 LONGITUDE 13.730 +/- 0.022 ***
 FOCAL DEPTH 26.7 +/- 3.2 KM ***

STA	ARR.	TIME	RES.	WEIGHT	DIST.	AZIMUTH	
GBD	P	07 48 15.50	0.07	30.5	90.1	31.3	P UP
GBD	S	07 48 26.41	-0.05	0.3	90.1	31.3	
VNY	P	07 48 17.20	0.20	27.5	100.7	315.2	P DOWN
VNY	S	07 48 29.34	0.11	0.3	100.7	315.2	
HFS	P	07 48 24.58	-0.10	17.8	152.2	359.3	P UP
TBY	P	07 48 24.66	-0.39	17.5	154.8	341.1	P UP
VIM	P	07 48 27.05	-0.40	6.8	172.6	128.4	P DOWN
SLL	P	07 48 29.93	0.12	6.0	191.7	353.2	
NYK	P	07 48 30.63	0.41	5.9	195.0	83.5	
HRN	P	07 48 34.59	0.39	2.1	227.3	42.2	
KTB	P	07 48 42.18	-0.17	1.5	293.4	28.1	P UP

INPUT DATA FOR FAULT PLANE SOLUTION

STN	DIST.	AZIMUTH	OMEGA(PZ)	OMEGA(SZ)
	KM	DEGREES	METER-SEC	METER-SEC
GBD	90.	31.3	+ 0.47E-07	0.97E-07
VNY	101.	315.2	- 0.71E-07	0.16E-06
VIM	173.	128.4	- 0.29E-07	0.12E-06
NYK	195.	83.5	0.20E-07	0.25E-06
HRN	227.	42.3	0.24E-07	0.99E-07
KTB	293.	28.1	+ 0.18E-07	0.11E-06
HFS	152.	359.3	+ 0.00E+00	0.00E+00
TBY	155.	341.1	+ 0.00E+00	0.00E+00

DYNAMIC SOURCE PARAMETERS

SIZE MEASURES

SEISMIC MOMENT: 0.383E+14 Nm
 LOCAL MAGNITUDE: 3.5

SHEAR WAVE CORNER FREQUENCY RANGE AT CLOSE DISTANCES (150km)
 5.9Hz - 9.7Hz (7.8Hz)

FAULT RADIUS RANGE 71m - 116m (88m)

STRESS DROP RANGE 10.47MPa - 46.53MPa (24.19MPa)

RANGE OF THE PEAK SLIP AT THE FAULT 30.7mm - 83.1mm (53.7mm)

861102 0748 0.7 58.770 13.730 26.7 3.5 Lake Vaernern
FOR THE BEST FITTING MECHANISM

THE ORIENTATION OF THE RELAXED STRESS

	AZIMUTH	DIP
P-AXIS	112.	-18. degrees
T-AXIS	27.	15.

THE HORIZONTAL DEVIATORIC STRESS AS GIVEN BY THE P- AND T-AXES
THE AZIMUTH OF COMPRESSION -65 degrees
THE RELATIVE SIZE 0.92

THE TWO POSSIBLE FAULT PLANES

	STRIKE	DIP	SLIP
PLANE A	70.	113.	-2. degrees
PLANE B	159.	88.	157.

THE NORMAL DIRECTIONS OF THE FAULT PLANES

	AZIMUTH	DIP
PLANE A	340.	23. degrees
PLANE B	249.	2.

STRIKE SLIP FAULTING DOMINATES

STATISTICAL INFORMATION

OF 6 FIRST MOTION POLARITY OBSERVATIONS
AT LEAST 6 ARE REQUIRED TO FIT

THE OPTIMUM MECHANISM HAS 0 POLARITY MISFITS

AMPLITUDES FOR P AND S AT 6 STATIONS ARE USED
ONLY MECHANISMS GIVING AN ESTIMATED STANDARD
DEVIATION OF THE AMPLITUDE ERROR FACTOR OF LESS
THAN 2.00 FOR SINGLE P-WAVE OBSERVATIONS ARE
TAKEN AS ACCEPTABLE AND INCLUDED IN THE FIGURES

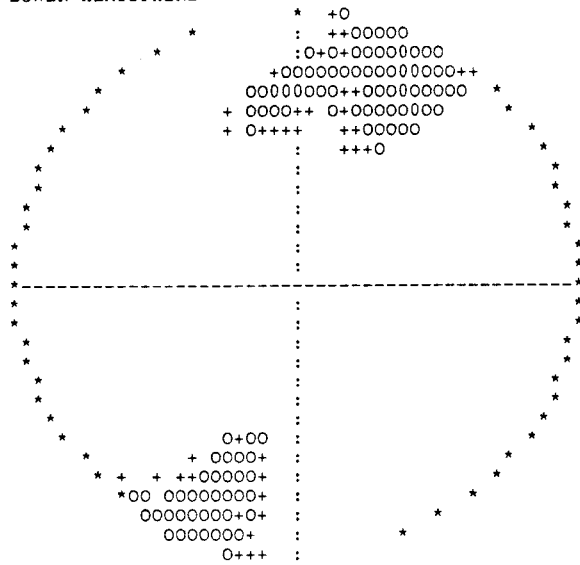
2.21 % OF ALL MECHANISMS ARE ACCEPTABLE
5.8 % ACCEPTABLE DUE TO FIRST MOTION OBSERVATIONS
37.9 % OF THESE FITTED ALSO THE AMPLITUDES
THE PART OF WELL FITTING PLANES IS 15.8%

THE AMPLITUDE FIT OF THE OPTIMAL MECHANISM
GIVES A MEAN ERROR FACTOR OF 1.40
THIS CORRESPONDS TO A STANDARD DEVIATION FACTOR OF 1.51
FOR SINGLE P-WAVE OBSERVATIONS

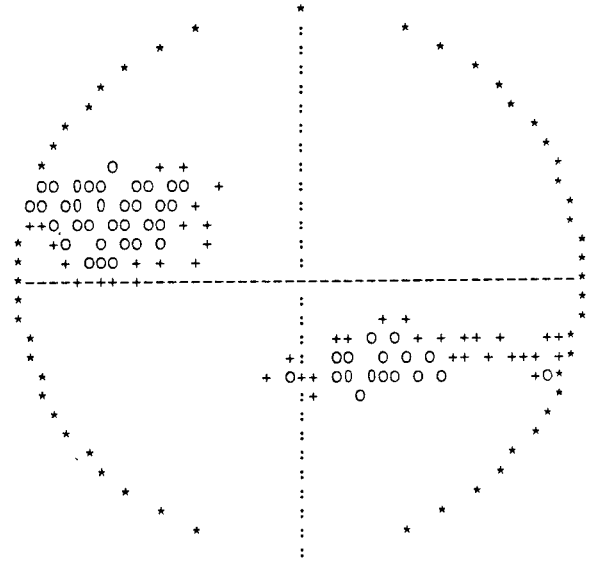
THE DOUBLE COUPLE SOLUTION IS SIGNIFICANT
AT 40 % LEVEL
(F-VALUE: $F(11, 8) = 1.21$)

861102 0748 0.7 58.770 13.730 26.7 3.5 Lake Vaernern

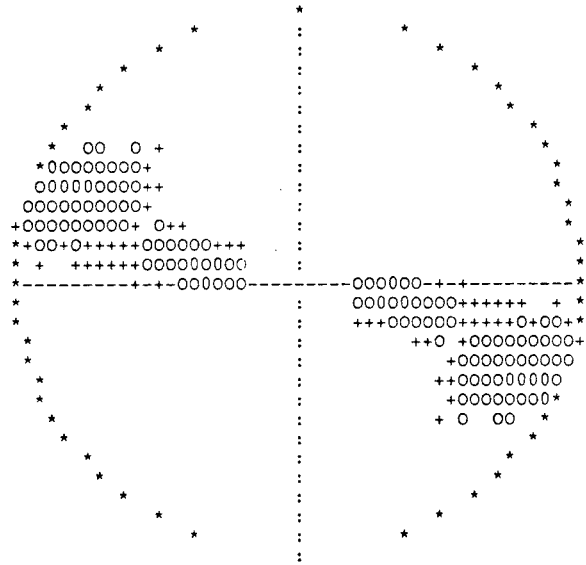
T-AXIS ORIENTATIONS
EQUAL AREA PROJECTION
LOWER HEMISPHERE



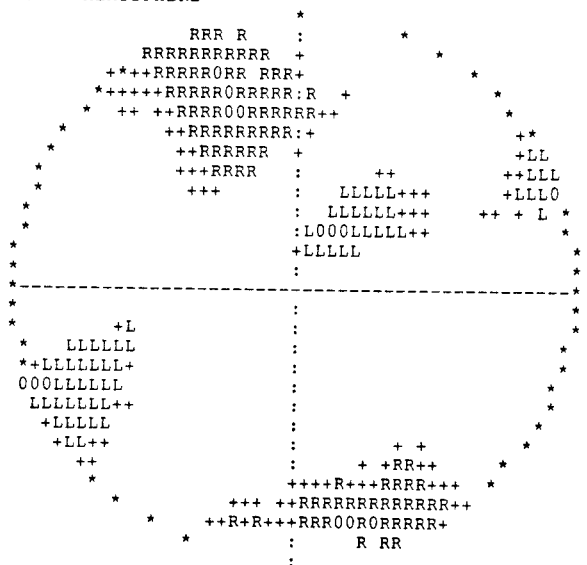
P-AXIS ORIENTATIONS
EQUAL AREA PROJECTION
LOWER HEMISPHERE



HORIZONTAL DEVIATORIC STRESS
RELATIVE SIZE AND
ORIENTATION OF COMPRESSION



FAULT PLANE ORIENTATIONS
GIVEN BY NORMAL VECTORS
EQUAL AREA PROJECTION
LOWER HEMISPHERE



870107 193742.9 58.435 13.935 21.9 2.1 Skoevde aftershock

ORIGIN TIME 87 01 07 19H 37M 43.0S +/- 0.19S ***
 LATITUDE 58.446 +/- 0.014 DEG. 11.km from n:o 11
 LONGITUDE 13.949 +/- 0.031 Billingen EM.
 FOCAL DEPTH 21.9 +/- 3.1 KM ***

STA	ARR.	TIME	RES.	WEIGHT	DIST.	AZIMUTH		
GBD	P	19 38	1.96	0.13	23.5	118.0	16.9	P UP
GBD	S	19 38	15.49	-0.49	0.3	118.0	16.9	
VNY	P	19 38	4.50	-0.06	20.2	136.2	322.2	P DOWN
VNY	S	19 38	21.19	0.40	0.3	136.2	322.2	
VIM	P	19 38	5.28	-0.09	19.3	141.7	120.4	
HFS	P	19 38	12.03	-0.14	6.1	188.8	355.7	
NYK	P	19 38	12.10	-0.23	6.1	190.1	72.4	
NYK	S	19 38	33.99	-0.62	0.1	190.1	72.4	
ALR	P	19 38	13.96	0.41	5.7	200.0	143.2	

INPUT DATA FOR FAULT PLANE SOLUTION

STN	DIST.	AZIMUTH	OMEGA(PZ)	OMEGA(SZ)
	KM	DEGREES	METER-SEC	METER-SEC
GBD	119.	16.8	+ 0.49E-09	0.79E-08
VNY	137.	322.4	- 0.62E-09	0.12E-08
VIM	141.	120.1	0.38E-09	0.19E-08
NYK	190.	72.2	0.75E-09	0.18E-08
ALR	199.	143.1	0.41E-09	0.13E-08
HRN	248.	34.5	0.25E-09	0.15E-08

DYNAMIC SOURCE PARAMETERS

SIZE MEASURES

SEISMIC MOMENT: 0.122E+13 Nm
 LOCAL MAGNITUDE: 2.1

SHEAR WAVE CORNER FREQUENCY RANGE AT CLOSE DISTANCES (150km)
 3.7Hz - 5.4Hz (4.5Hz)

FAULT RADIUS RANGE 127m - 186m (153m)

STRESS DROP RANGE 0.08MPa - 0.26MPa (0.15MPa)

RANGE OF THE PEAK SLIP AT THE FAULT 0.4mm - 0.8mm (0.6mm)

870107 193742.9 58.435 13.935 21.9 2.1 Skoevde aftershock
FOR THE BEST FITTING MECHANISM

THE ORIENTATION OF THE RELAXED STRESS

	AZIMUTH	DIP
P-AXIS	149.	-41. degrees
T-AXIS	69.	12.

THE HORIZONTAL DEVIATORIC STRESS AS GIVEN BY THE P- AND T-AXES
THE AZIMUTH OF COMPRESSION -25 degrees
THE RELATIVE SIZE 0.76

THE TWO POSSIBLE FAULT PLANES

	STRIKE	DIP	SLIP
PLANE A	118.	127.	-24. degrees
PLANE B	193.	71.	140.

THE NORMAL DIRECTIONS OF THE FAULT PLANES

	AZIMUTH	DIP
PLANE A	28.	37. degrees
PLANE B	283.	19.

STRIKE SLIP FAULTING DOMINATES

STATISTICAL INFORMATION

OF 2 FIRST MOTION POLARITY OBSERVATIONS
AT LEAST 2 ARE REQUIRED TO FIT

THE OPTIMUM MECHANISM HAS 0 POLARITY MISFITS

AMPLITUDES FOR P AND S AT 6 STATIONS ARE USED
ONLY MECHANISMS GIVING AN ESTIMATED STANDARD
DEVIATION OF THE AMPLITUDE ERROR FACTOR OF LESS
THAN 2.00 FOR SINGLE P-WAVE OBSERVATIONS ARE
TAKEN AS ACCEPTABLE AND INCLUDED IN THE FIGURES

3.92 % OF ALL MECHANISMS ARE ACCEPTABLE
24.6 % ACCEPTABLE DUE TO FIRST MOTION OBSERVATIONS
15.9 % OF THESE FITTED ALSO THE AMPLITUDES
THE PART OF WELL FITTING PLANES IS 17.7%

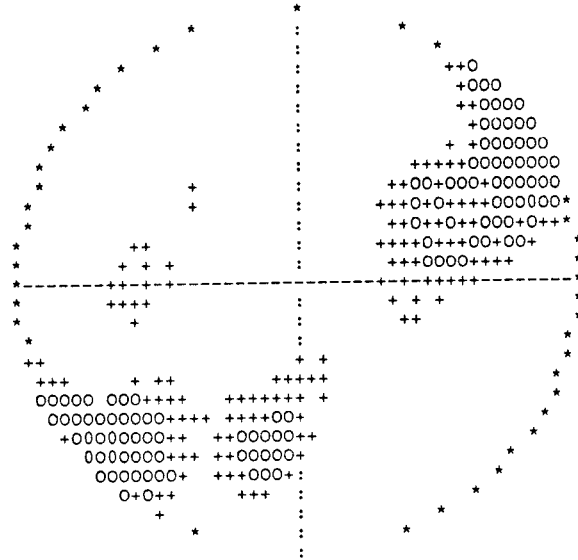
THE AMPLITUDE FIT OF THE OPTIMAL MECHANISM
GIVES A MEAN ERROR FACTOR OF 1.38
THIS CORRESPONDS TO A STANDARD DEVIATION FACTOR OF 1.49
FOR SINGLE P-WAVE OBSERVATIONS

THE DOUBLE COUPLE SOLUTION IS SIGNIFICANT
AT 15 % LEVEL
(F-VALUE: $F(11, 8) = 2.09$)

870107 193742.9 58.435 13.935 21.9 2.1 Skoevde aftershock

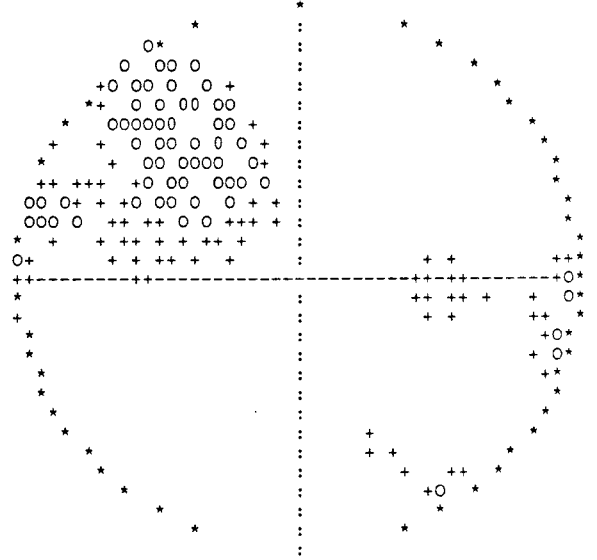
T-AXIS ORIENTATIONS
EQUAL AREA PROJECTION
LOWER HEMISPHERE

I00719380



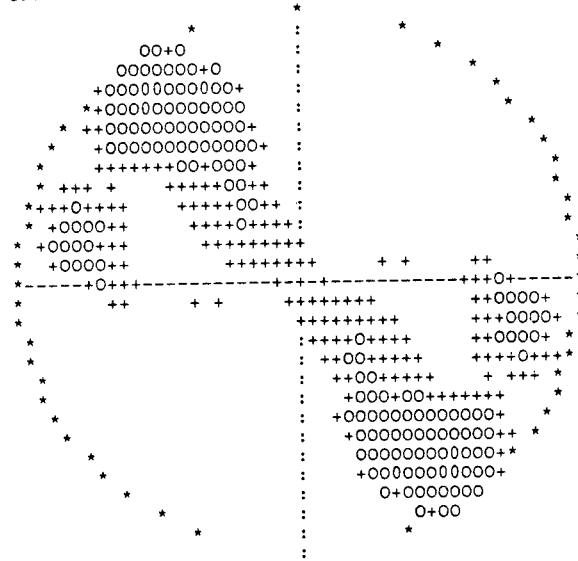
P-AXIS ORIENTATIONS
EQUAL AREA PROJECTION
LOWER HEMISPHERE

I00719380



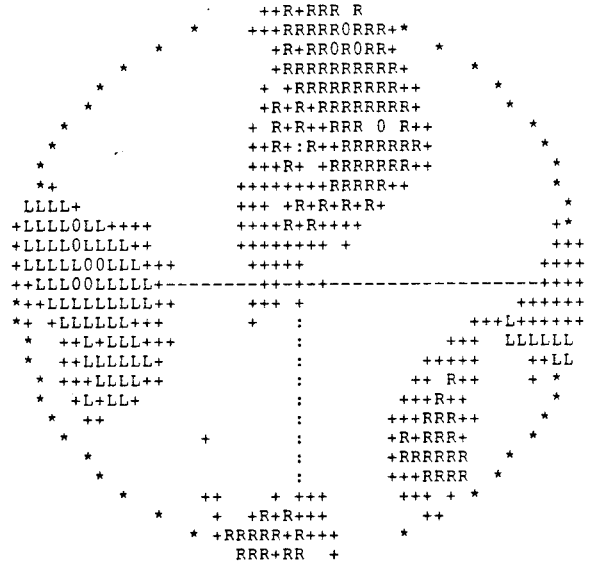
HORIZONTAL DEVIATORIC STRESS
RELATIVE SIZE AND
ORIENTATION OF COMPRESSION

I00719380



FAULT PLANE ORIENTATIONS
GIVEN BY NORMAL VECTORS
EQUAL AREA PROJECTION
LOWER HEMISPHERE

I00719380



870129 100210.5 58.433 13.975 (18.0) 1.4 Skoevde aftershock

ORIGIN TIME 87 01 29 10H 02M 10.2S +/- 0.54S *
 LATITUDE 58.432 +/- 0.023 DEG. 13.km from n:o 11
 LONGITUDE 13.998 +/- 0.040 Billingen EM.
 FOCAL DEPTH 18.1 +/- 7.6 KM ***

STA	ARR.	TIME	RES.	WEIGHT	DIST.	AZIMUTH
GBD	P	10 02 29.60	0.11	22.8	121.6	15.8
GBD	S	10 02 43.25	-0.86	0.3	121.6	15.8
VIM	P	10 02 32.08	-0.01	19.8	138.5	119.2
VIM	S	10 02 49.80	0.97	0.3	138.5	119.2
VNY	P	10 02 32.30	-0.07	19.5	140.3	322.9
VNY	S	10 02 48.93	-0.42	0.3	140.3	322.9
NYK	P	10 02 39.71	-0.11	6.1	190.1	71.1
NYK	S	10 03 1.08	-1.41	0.1	190.1	71.1
ALR	P	10 02 41.08	0.40	5.8	195.9	142.8

INPUT DATA FOR FAULT PLANE SOLUTION

STN	DIST.	AZIMUTH	OMEGA(PZ)	OMEGA(SZ)
	KM	DEGREES	METER-SEC	METER-SEC
GBD	119.	15.6	0.22E-09	0.86E-09
VNY	139.	322.0	0.14E-09	0.41E-09
VIM	139.	120.2	0.20E-09	0.41E-09
NYK	188.	71.7	0.12E-09	0.88E-09
ALR	197.	143.5	0.18E-09	0.33E-09
HRN	248.	34.0	0.13E-09	0.49E-09

DYNAMIC SOURCE PARAMETERS

SIZE MEASURES

SEISMIC MOMENT: 0.237E+12 Nm
 LOCAL MAGNITUDE: 1.4

SHEAR WAVE CORNER FREQUENCY RANGE AT CLOSE DISTANCES (150km)
 4.8Hz - 8.2Hz (6.3Hz)

FAULT RADIUS RANGE 84m - 143m (109m)

STRESS DROP RANGE 0.03MPa - 0.17MPa (0.08MPa)

RANGE OF THE PEAK SLIP AT THE FAULT 0.1mm - 0.4mm (0.2mm)

870129 100210.5 58.433 13.975 (18.0) 1.4 Skoevde aftershock
FOR THE BEST FITTING MECHANISM

THE ORIENTATION OF THE RELAXED STRESS

	AZIMUTH	DIP
P-AXIS	44.	-6. degrees
T-AXIS	133.	8.

THE HORIZONTAL DEVIATORIC STRESS AS GIVEN BY THE P- AND T-AXES
THE AZIMUTH OF COMPRESSION 43 degrees
THE RELATIVE SIZE 0.98

THE TWO POSSIBLE FAULT PLANES

	STRIKE	DIP	SLIP
PLANE A	268.	100.	179. degrees
PLANE B	178.	91.	10.

THE NORMAL DIRECTIONS OF THE FAULT PLANES

	AZIMUTH	DIP
PLANE A	178.	10. degrees
PLANE B	88.	1.

STRIKE SLIP FAULTING DOMINATES

STATISTICAL INFORMATION

OF 0 FIRST MOTION POLARITY OBSERVATIONS
AT LEAST 0 ARE REQUIRED TO FIT

THE OPTIMUM MECHANISM HAS 0 POLARITY MISFITS

AMPLITUDES FOR P AND S AT 6 STATIONS ARE USED
ONLY MECHANISMS GIVING AN ESTIMATED STANDARD
DEVIATION OF THE AMPLITUDE ERROR FACTOR OF LESS
THAN 2.00 FOR SINGLE P-WAVE OBSERVATIONS ARE
TAKEN AS ACCEPTABLE AND INCLUDED IN THE FIGURES

16.86 % OF ALL MECHANISMS ARE ACCEPTABLE
100.0 % ACCEPTABLE DUE TO FIRST MOTION OBSERVATIONS
16.9 % OF THESE FITTED ALSO THE AMPLITUDES
THE PART OF WELL FITTING PLANES IS 35.3%

THE AMPLITUDE FIT OF THE OPTIMAL MECHANISM
GIVES A MEAN ERROR FACTOR OF 1.27
THIS CORRESPONDS TO A STANDARD DEVIATION FACTOR OF 1.34
FOR SINGLE P-WAVE OBSERVATIONS

THE DOUBLE COUPLE SOLUTION IS SIGNIFICANT
AT 7 % LEVEL
(F-VALUE: $F(11, 8) = 2.74$)

870202 094654.5 61.157 16.652 20.6 2.0 SV Soederhamn

ORIGIN TIME 87 02 02 09H 46M 54.5S +/- 1.33S **:
 LATITUDE 61.160 +/- 0.073 DEG. 21.km from n:o 35
 LONGITUDE 16.657 +/- 0.152 S Ljusne 5787:20
 FOCAL DEPTH 20.4 +/- 1.8 KM ***

STA	ARR.	TIME	RES.	WEIGHT	DIST.	AZIMUTH	
KTB	S	09 47	3.21	0.18	0.5	22.7	242.5
KTB	P	09 46	59.38	0.00	69.0	22.7	242.5
HRN	P	09 47	10.93	0.00	27.2	102.0	185.3
HRN	S	09 47	22.91	-0.34	0.3	102.0	185.3
SLL	P	09 47	24.77	-0.03	5.8	197.2	248.7
HFS	P	09 47	25.01	0.04	5.7	198.5	236.1
HFS	S	09 47	47.77	-0.36	0.1	198.5	236.1
GBD	S	09 47	54.13	0.78	0.0	222.8	212.4

P UP

INPUT DATA FOR FAULT PLANE SOLUTION

STN	DIST.	AZIMUTH	OMEGA(PZ)	OMEGA(SZ)
	KM	DEGREES	METER-SEC	METER-SEC
KTB	22.	242.2	+ 0.32E-09	0.35E-08
HRN	102.	185.1	0.31E-09	0.11E-08
GBD	223.	212.3	0.38E-09	0.72E-09
NYK	251.	174.2	0.22E-09	0.15E-08
VNY	303.	231.5	0.37E-09	0.13E-08

DYNAMIC SOURCE PARAMETERS

SIZE MEASURES

SEISMIC MOMENT: 0.100E+13 Nm
 LOCAL MAGNITUDE: 2.0

SHEAR WAVE CORNER FREQUENCY RANGE AT CLOSE DISTANCES (150km)
 7.9Hz -21.3Hz (11.8Hz)

FAULT RADIUS RANGE 32m - 87m (58m)

STRESS DROP RANGE 0.66MPa - 12.93MPa (2.20MPa)

RANGE OF THE PEAK SLIP AT THE FAULT 1.5mm - 10.6mm (3.2mm)

870202 094654.5 61.157 16.652 20.6 2.0 SV Soederhamn
FOR THE BEST FITTING MECHANISM

THE ORIENTATION OF THE RELAXED STRESS

	AZIMUTH	DIP
P-AXIS	54.	-35. degrees
T-AXIS	132.	16.

THE HORIZONTAL DEVIATORIC STRESS AS GIVEN BY THE P- AND T-AXES
THE AZIMUTH OF COMPRESSION 46 degrees
THE RELATIVE SIZE 0.78

THE TWO POSSIBLE FAULT PLANES

	STRIKE	DIP	SLIP
PLANE A	267.	127.	195. degrees
PLANE B	186.	78.	38.

THE NORMAL DIRECTIONS OF THE FAULT PLANES

	AZIMUTH	DIP
PLANE A	177.	37. degrees
PLANE B	276.	12.

STRIKE SLIP FAULTING DOMINATES

STATISTICAL INFORMATION

OF 1 FIRST MOTION POLARITY OBSERVATIONS
AT LEAST 1 ARE REQUIRED TO FIT

THE OPTIMUM MECHANISM HAS 0 POLARITY MISFITS

AMPLITUDES FOR P AND S AT 5 STATIONS ARE USED
ONLY MECHANISMS GIVING AN ESTIMATED STANDARD
DEVIATION OF THE AMPLITUDE ERROR FACTOR OF LESS
THAN 2.00 FOR SINGLE P-WAVE OBSERVATIONS ARE
TAKEN AS ACCEPTABLE AND INCLUDED IN THE FIGURES

5.31 % OF ALL MECHANISMS ARE ACCEPTABLE
50.0 % ACCEPTABLE DUE TO FIRST MOTION OBSERVATIONS
10.5 % OF THESE FITTED ALSO THE AMPLITUDES
THE PART OF WELL FITTING PLANES IS 21.3%

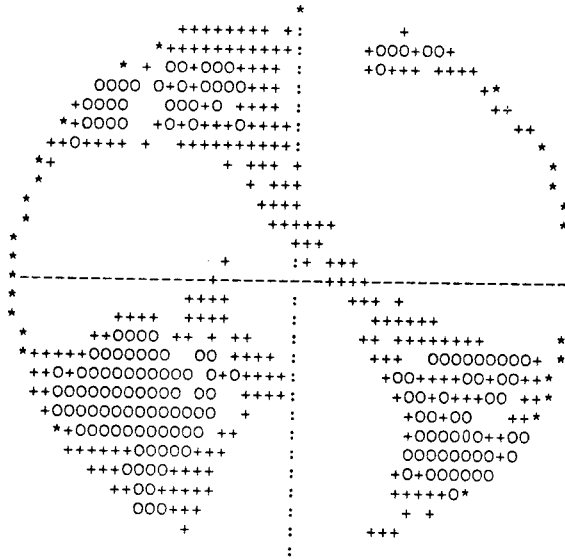
THE AMPLITUDE FIT OF THE OPTIMAL MECHANISM
GIVES A MEAN ERROR FACTOR OF 1.29
THIS CORRESPONDS TO A STANDARD DEVIATION FACTOR OF 1.38
FOR SINGLE P-WAVE OBSERVATIONS

THE DOUBLE COUPLE SOLUTION IS SIGNIFICANT
AT 2 % LEVEL
(F-VALUE: $F(9, 6) = 5.71$)

870202 094654.5 61.157 16.652 20.6 2.0 SV Soederhamm

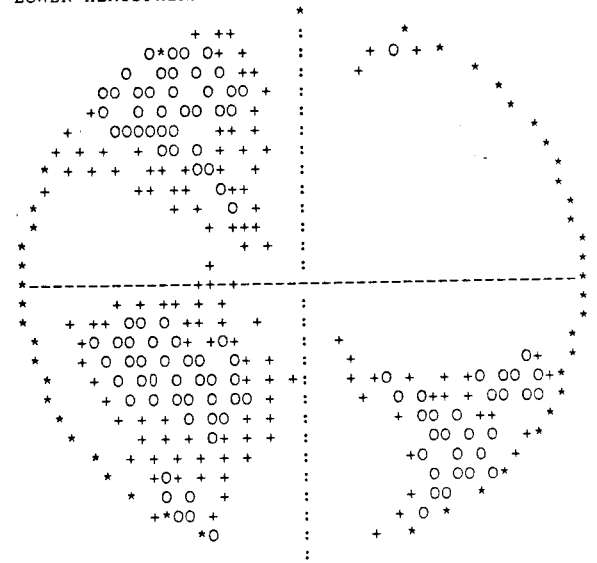
T-AXIS ORIENTATIONS
EQUAL AREA PROJECTION
LOWER HEMISPHERE

I03309471



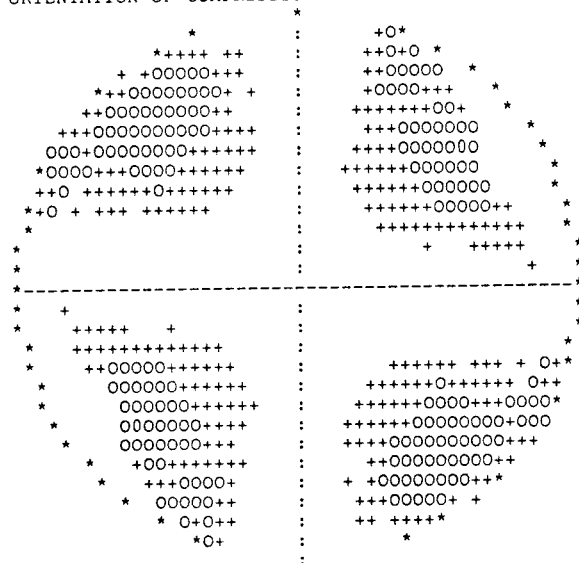
P-AXIS ORIENTATIONS
EQUAL AREA PROJECTION
LOWER HEMISPHERE

I03309471



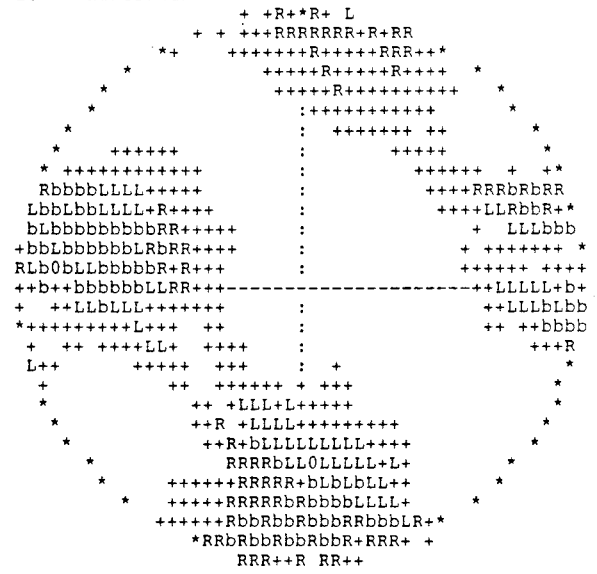
HORIZONTAL DEVIATORIC STRESS
RELATIVE SIZE AND
ORIENTATION OF COMPRESSION

I03309471



FAULT PLANE ORIENTATIONS
GIVEN BY NORMAL VECTORS
EQUAL AREA PROJECTION
LOWER HEMISPHERE

I03309471



870218 155258.6 60.070 12.525 20.2 1.9 Vermland

ORIGIN TIME 87 02 18 15H 52M 58.6S +/- 0.20S **
 LATITUDE 60.066 +/- 0.010 DEG. 30.km from n:o 99
 LONGITUDE 12.529 +/- 0.033 ***
 FOCAL DEPTH 20.3 +/- 4.5 KM ***

STA	ARR.	TIME	RES.	WEIGHT	DIST.	AZIMUTH	
SLL	P	15 53 9.22	0.04	40.8	62.9	43.8	P UP
SLL	S	15 53 17.54	0.48	0.4	62.9	43.8	
HFS	P	15 53 9.63	0.09	39.7	65.3	83.3	P DOWN
HFS	S	15 53 18.19	0.50	0.4	65.3	83.3	
VNY	P	15 53 10.86	-0.05	35.9	74.5	182.1	
VNY	S	15 53 20.03	-0.07	0.4	74.5	182.1	
GBD	P	15 53 19.48	-0.17	20.8	132.9	120.1	
GBD	S	15 53 35.66	0.16	0.3	132.9	120.1	
HRN	P	15 53 32.40	0.61	2.2	220.8	83.1	
HRN	S	15 53 57.50	0.55	0.0	220.8	83.1	
KTB	P	15 53 33.08	-0.35	2.0	234.1	60.1	
NYK	S	15 54 11.92	0.42	0.0	288.5	114.3	
VIM	P	15 53 44.52	0.02	1.3	323.8	140.3	

INPUT DATA FOR FAULT PLANE SOLUTION

STN	DIST.	AZIMUTH	OMEGA(PZ)	OMEGA(SZ)
	KM	DEGREES	METER-SEC	METER-SEC
VNY	74.	181.7	0.41E-09	0.25E-08
GBD	133.	120.0	0.59E-09	0.23E-08
HRN	221.	83.1	0.20E-09	0.13E-08
KTB	235.	60.1	0.25E-09	0.10E-08
NYK	289.	114.3	0.49E-09	0.16E-08
HFS	66.	83.3	- 0.00E+00	0.00E+00
SLL	63.	44.1	+ 0.00E+00	0.00E+00

DYNAMIC SOURCE PARAMETERS

SIZE MEASURES

SEISMIC MOMENT: 0.712E+12 Nm

LOCAL MAGNITUDE: 1.9

SHEAR WAVE CORNER FREQUENCY RANGE AT CLOSE DISTANCES (150km)
 7.2Hz -11.8Hz (9.3Hz)

FAULT RADIUS RANGE 58m - 95m (74m)

STRESS DROP RANGE 0.35MPa - 1.56MPa (0.76MPa)

RANGE OF THE PEAK SLIP AT THE FAULT 0.9mm - 2.3mm (1.4mm)

870218 155258.6 60.070 12.525 20.2 1.9 Vermland
FOR THE BEST FITTING MECHANISM

THE ORIENTATION OF THE RELAXED STRESS

	AZIMUTH	DIP
P-AXIS	118.	-1. degrees
T-AXIS	28.	28.

THE HORIZONTAL DEVIATORIC STRESS AS GIVEN BY THE P- AND T-AXES
THE AZIMUTH OF COMPRESSION -62 degrees
THE RELATIVE SIZE 0.89

THE TWO POSSIBLE FAULT PLANES

	STRIKE	DIP	SLIP
PLANE A	70.	110.	20. degrees
PLANE B	167.	109.	159.

THE NORMAL DIRECTIONS OF THE FAULT PLANES

	AZIMUTH	DIP
PLANE A	340.	20. degrees
PLANE B	77.	19.

STRIKE SLIP FAULTING DOMINATES

STATISTICAL INFORMATION

OF 2 FIRST MOTION POLARITY OBSERVATIONS
AT LEAST 2 ARE REQUIRED TO FIT

THE OPTIMUM MECHANISM HAS 0 POLARITY MISFITS

AMPLITUDES FOR P AND S AT 5 STATIONS ARE USED
ONLY MECHANISMS GIVING AN ESTIMATED STANDARD
DEVIATION OF THE AMPLITUDE ERROR FACTOR OF LESS
THAN 2.00 FOR SINGLE P-WAVE OBSERVATIONS ARE
TAKEN AS ACCEPTABLE AND INCLUDED IN THE FIGURES

7.25 % OF ALL MECHANISMS ARE ACCEPTABLE
18.4 % ACCEPTABLE DUE TO FIRST MOTION OBSERVATIONS
39.4 % OF THESE FITTED ALSO THE AMPLITUDES
THE PART OF WELL FITTING PLANES IS 40.0%

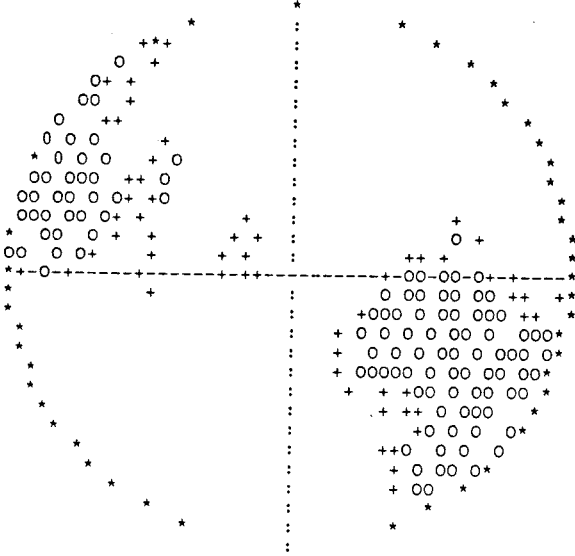
THE AMPLITUDE FIT OF THE OPTIMAL MECHANISM
GIVES A MEAN ERROR FACTOR OF 1.22
THIS CORRESPONDS TO A STANDARD DEVIATION FACTOR OF 1.30
FOR SINGLE P-WAVE OBSERVATIONS

THE DOUBLE COUPLE SOLUTION IS SIGNIFICANT
AT 5 % LEVEL
(F-VALUE: $F(9, 6) = 3.98$)

870218 155258.6 60.070 12.525 20.2 1.9 Vermland

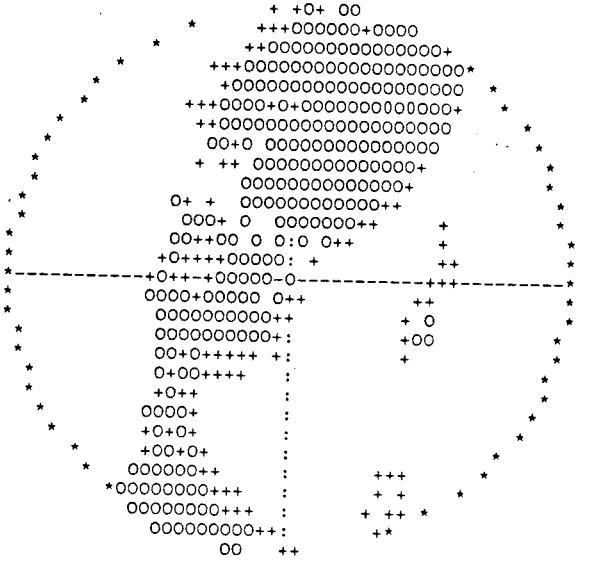
P-AXIS ORIENTATIONS
EQUAL AREA PROJECTION
LOWER HEMISPHERE

I04915531



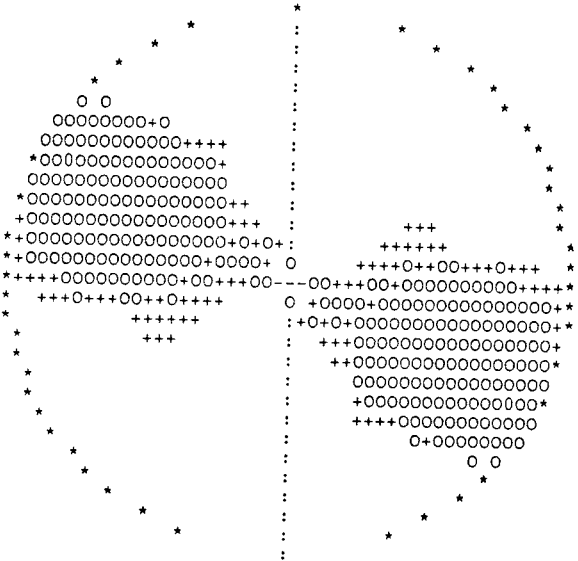
T-AXIS ORIENTATIONS
EQUAL AREA PROJECTION
LOWER HEMISPHERE

I04915531



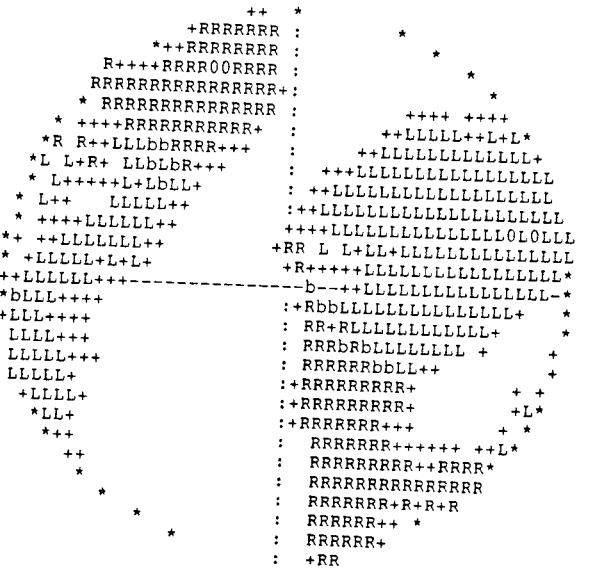
HORIZONTAL DEVIATORIC STRESS
RELATIVE SIZE AND
ORIENTATION OF COMPRESSION

I04915531



FAULT PLANE ORIENTATIONS
GIVEN BY NORMAL VECTORS
EQUAL AREA PROJECTION
LOWER HEMISPHERE

I04915531



870317 023734.2 60.156 15.858 5.3 1.7 Bergslagen

ORIGIN TIME 87 03 17 02H 37M 34.2S +/- 0.08S ***
 LATITUDE 60.156 +/- 0.009 DEG. 9.km from n:o 12
 LONGITUDE 15.858 +/- 0.011 Avesta EM.
 FOCAL DEPTH 5.3 +/- 3.5 KM ***

STA	ARR.	TIME	RES.	WEIGHT	DIST.	AZIMUTH	
HRN	P	02 37 40.19	-0.04	56.8	36.4	73.0	P DOWN
HRN	S	02 37 44.53	-0.15	0.5	36.4	73.0	
KTB	P	02 37 51.39	0.14	26.7	104.2	12.8	
KTB	S	02 38 3.63	-0.17	0.3	104.2	12.8	
GBD	P	02 37 51.87	0.16	26.0	107.0	223.8	
HFS	P	02 37 53.75	-0.13	23.1	120.3	269.8	
HFS	S	02 38 7.63	-0.72	0.3	120.3	269.8	
SLL	P	02 37 57.81	-0.06	18.8	144.9	285.3	P DOWN
NYK	P	02 37 59.25	-0.04	17.6	154.1	152.5	
VNY	P	02 38 7.10	-0.19	2.4	207.6	247.6	
VIM	P	02 38 14.51	0.15	1.7	264.3	178.1	

INPUT DATA FOR FAULT PLANE SOLUTION

STN	DIST.	AZIMUTH	OMEGA(PZ)	OMEGA(SZ)
	KM	DEGREES	METER-SEC	METER-SEC
HRN	37.	72.2	- 0.36E-09	0.15E-08
KTB	105.	12.9	0.22E-09	0.15E-08
GBD	106.	223.9	0.17E-09	0.77E-09
NYK	154.	152.3	0.49E-09	0.16E-08
VNY	207.	247.7	0.19E-09	0.89E-09
VIM	264.	178.0	0.54E-09	0.11E-08
SLL	145.	285.6	- 0.00E+00	0.00E+00

DYNAMIC SOURCE PARAMETERS

SIZE MEASURES

SEISMIC MOMENT: 0.525E+12 Nm

LOCAL MAGNITUDE: 1.7

SHEAR WAVE CORNER FREQUENCY RANGE AT CLOSE DISTANCES (150km)
 6.4Hz -12.6Hz (8.8Hz)

FAULT RADIUS RANGE 54m - 107m (78m)

STRESS DROP RANGE 0.18MPa - 1.40MPa (0.48MPa)

RANGE OF THE PEAK SLIP AT THE FAULT 0.6mm - 2.5mm (1.2mm)

870317 023734.2 60.156 15.858 5.3 1.7 Bergslagen
 FOR THE BEST FITTING MECHANISM

THE ORIENTATION OF THE RELAXED STRESS

	AZIMUTH	DIP
P-AXIS	117.	-35. degrees
T-AXIS	163.	45.

THE HORIZONTAL DEVIATORIC STRESS AS GIVEN BY THE P- AND T-AXES
 THE AZIMUTH OF COMPRESSION -81 degrees
 THE RELATIVE SIZE 0.43

THE TWO POSSIBLE FAULT PLANES

	STRIKE	DIP	SLIP
PLANE A	-31.	154.	168. degrees
PLANE B	228.	95.	65.

THE NORMAL DIRECTIONS OF THE FAULT PLANES

	AZIMUTH	DIP
PLANE A	239.	64. degrees
PLANE B	138.	5.

STATISTICAL INFORMATION

OF 2 FIRST MOTION POLARITY OBSERVATIONS
 AT LEAST 2 ARE REQUIRED TO FIT

THE OPTIMUM MECHANISM HAS 0 POLARITY MISFITS

AMPLITUDES FOR P AND S AT 6 STATIONS ARE USED
 ONLY MECHANISMS GIVING AN ESTIMATED STANDARD
 DEVIATION OF THE AMPLITUDE ERROR FACTOR OF LESS
 THAN 2.00 FOR SINGLE P-WAVE OBSERVATIONS ARE
 TAKEN AS ACCEPTABLE AND INCLUDED IN THE FIGURES

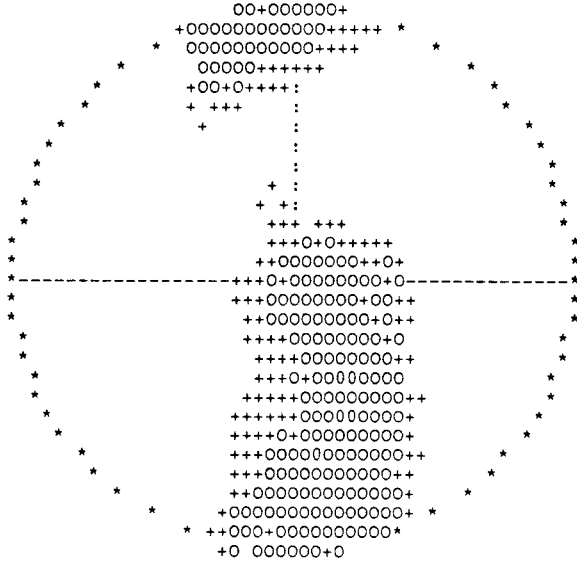
8.68 % OF ALL MECHANISMS ARE ACCEPTABLE
 32.3 % ACCEPTABLE DUE TO FIRST MOTION OBSERVATIONS
 26.9 % OF THESE FITTED ALSO THE AMPLITUDES
 THE PART OF WELL FITTING PLANES IS 37.2%

THE AMPLITUDE FIT OF THE OPTIMAL MECHANISM
 GIVES A MEAN ERROR FACTOR OF 1.35
 THIS CORRESPONDS TO A STANDARD DEVIATION FACTOR OF 1.44
 FOR SINGLE P-WAVE OBSERVATIONS

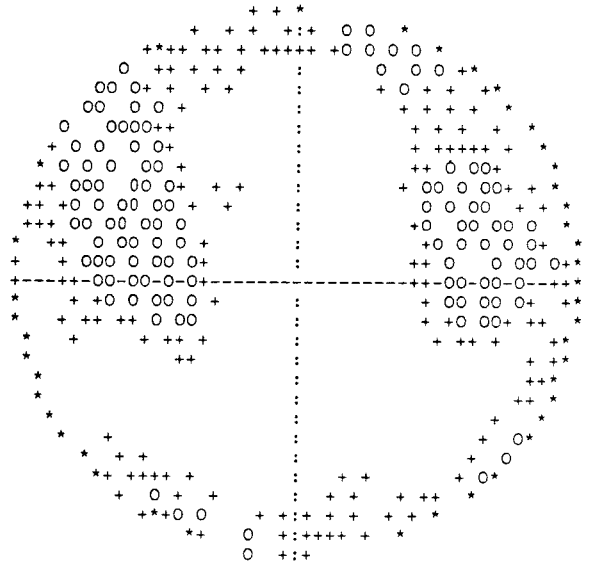
THE DOUBLE COUPLE SOLUTION IS SIGNIFICANT
 AT 18 % LEVEL
 (F-VALUE: $F(11, 8) = 1.93$)

870317 023734.2 60.156 15.858 5.3 1.7 Bergslagen

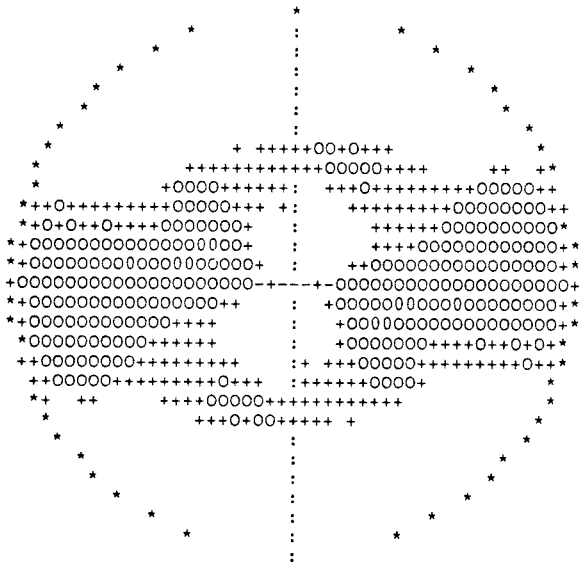
T-AXIS ORIENTATIONS
EQUAL AREA PROJECTION I07602374
LOWER HEMISPHERE



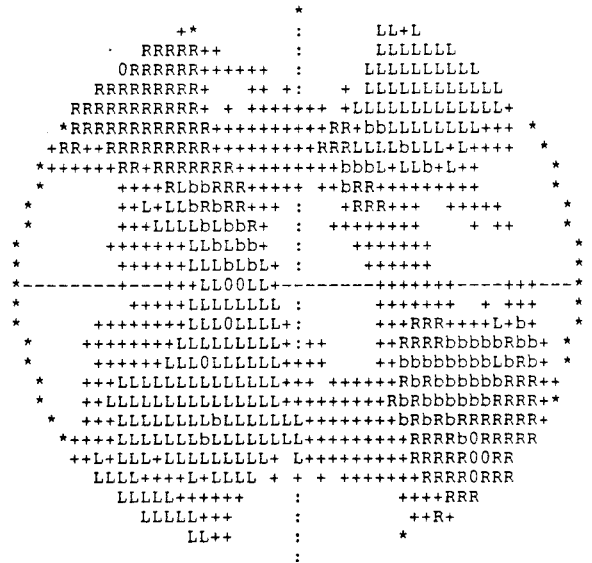
P-AXIS ORIENTATIONS
EQUAL AREA PROJECTION I07602374
LOWER HEMISPHERE



HORIZONTAL DEVIATORIC STRESS
RELATIVE SIZE AND
ORIENTATION OF COMPRESSION I07602374



FAULT PLANE ORIENTATIONS
GIVEN BY NORMAL VECTORS
EQUAL AREA PROJECTION I07602374
LOWER HEMISPHERE



870320 204211.7 58.426 13.978 19.3 2.0 Skoevde aftershock
FOR THE BEST FITTING MECHANISM

THE ORIENTATION OF THE RELAXED STRESS

	AZIMUTH	DIP
P-AXIS	113.	5. degrees
T-AXIS	26.	-35.

THE HORIZONTAL DEVIATORIC STRESS AS GIVEN BY THE P- AND T-AXES
THE AZIMUTH OF COMPRESSION -66 degrees
THE RELATIVE SIZE 0.83

THE TWO POSSIBLE FAULT PLANES

	STRIKE	DIP	SLIP
PLANE A	64.	62.	-23. degrees
PLANE B	165.	70.	210.

THE NORMAL DIRECTIONS OF THE FAULT PLANES

	AZIMUTH	DIP
PLANE A	154.	28. degrees
PLANE B	255.	20.

STRIKE SLIP FAULTING DOMINATES

STATISTICAL INFORMATION

OF 2 FIRST MOTION POLARITY OBSERVATIONS
AT LEAST 2 ARE REQUIRED TO FIT

THE OPTIMUM MECHANISM HAS 0 POLARITY MISFITS

AMPLITUDES FOR P AND S AT 6 STATIONS ARE USED
ONLY MECHANISMS GIVING AN ESTIMATED STANDARD
DEVIATION OF THE AMPLITUDE ERROR FACTOR OF LESS
THAN 2.00 FOR SINGLE P-WAVE OBSERVATIONS ARE
TAKEN AS ACCEPTABLE AND INCLUDED IN THE FIGURES

5.98 % OF ALL MECHANISMS ARE ACCEPTABLE
24.2 % ACCEPTABLE DUE TO FIRST MOTION OBSERVATIONS
24.7 % OF THESE FITTED ALSO THE AMPLITUDES
THE PART OF WELL FITTING PLANES IS 22.8%

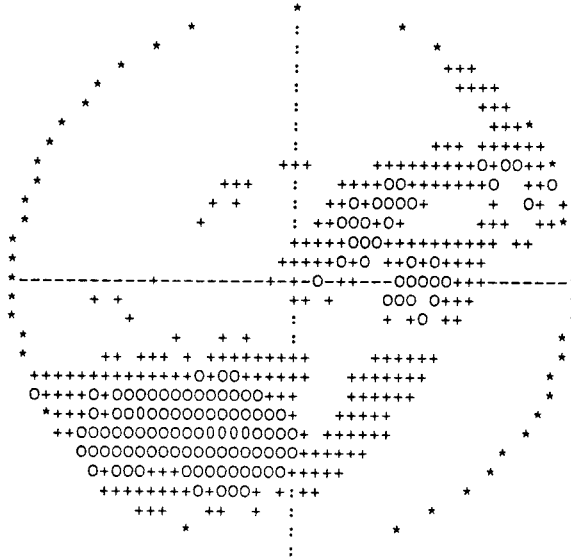
THE AMPLITUDE FIT OF THE OPTIMAL MECHANISM
GIVES A MEAN ERROR FACTOR OF 1.34
THIS CORRESPONDS TO A STANDARD DEVIATION FACTOR OF 1.43
FOR SINGLE P-WAVE OBSERVATIONS

THE DOUBLE COUPLE SOLUTION IS SIGNIFICANT
AT 31 % LEVEL
(F-VALUE: $F(11, 8) = 1.44$)

870320 204211.7 58.426 13.978 19.3 2.0 Skoevde aftershock

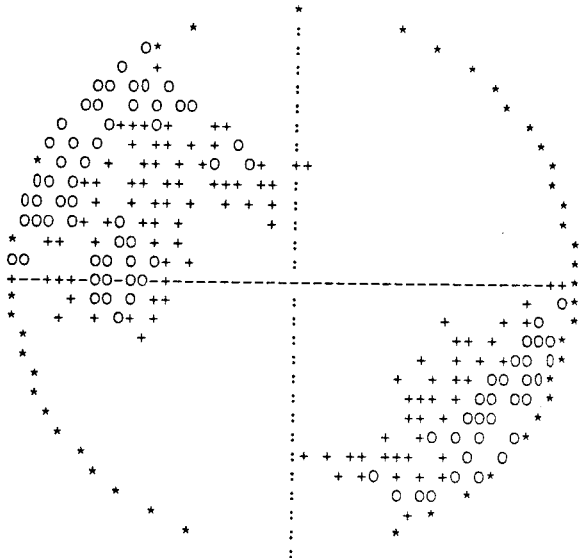
T-AXIS ORIENTATIONS
EQUAL AREA PROJECTION
LOWER HEMISPHERE

I07920423



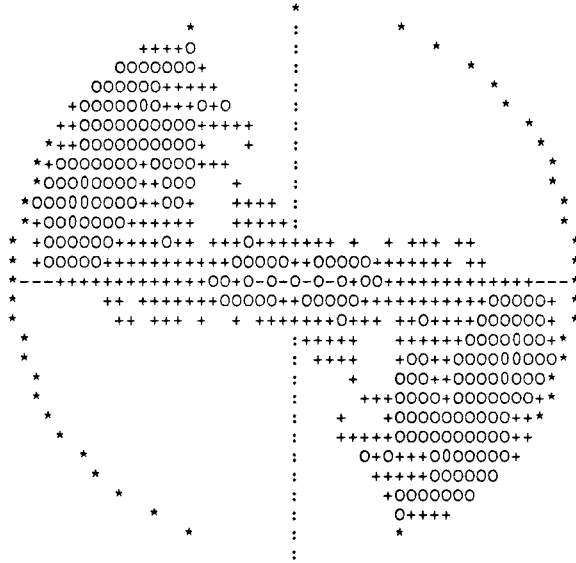
P-AXIS ORIENTATIONS
EQUAL AREA PROJECTION
LOWER HEMISPHERE

I07920423



HORIZONTAL DEVIATORIC STRESS
RELATIVE SIZE AND
ORIENTATION OF COMPRESSION

I07920423



FAULT PLANE ORIENTATIONS
GIVEN BY NORMAL VECTORS
EQUAL AREA PROJECTION
LOWER HEMISPHERE

I07920423



List of SKB reports

Annual Reports

1977-78

TR 121

KBS Technical Reports 1 – 120.

Summaries. Stockholm, May 1979.

1979

TR 79-28

The KBS Annual Report 1979.

KBS Technical Reports 79-01 – 79-27.
Summaries. Stockholm, March 1980.

1980

TR 80-26

The KBS Annual Report 1980.

KBS Technical Reports 80-01 – 80-25.
Summaries. Stockholm, March 1981.

1981

TR 81-17

The KBS Annual Report 1981.

KBS Technical Reports 81-01 – 81-16.
Summaries. Stockholm, April 1982.

1982

TR 82-28

The KBS Annual Report 1982.

KBS Technical Reports 82-01 – 82-27.
Summaries. Stockholm, July 1983.

1983

TR 83-77

The KBS Annual Report 1983.

KBS Technical Reports 83-01 – 83-76
Summaries. Stockholm, June 1984.

1984

TR 85-01

Annual Research and Development Report 1984

Including Summaries of Technical Reports Issued during 1984. (Technical Reports 84-01-84-19)
Stockholm June 1985.

1985

TR 85-20

Annual Research and Development Report 1985

Including Summaries of Technical Reports Issued during 1985. (Technical Reports 85-01-85-19)
Stockholm May 1986.

1986

TR86-31

SKB Annual Report 1986

Including Summaries of Technical Reports Issued during 1986
Stockholm, May 1987

Technical Reports

1987

TR 87-01

Radar measurements performed at the Klipperås study site

Seje Carlsten, Olle Olsson, Stefan Sehlstedt,
Leif Stenberg
Swedish Geological Co, Uppsala/Luleå
February 1987

TR 87-02

Fuel rod D07/B15 from Ringhals 2 PWR: Source material for corrosion/leach tests in groundwater Fuel rod/pellet characterization program part one

Roy Forsyth, Editor
Studsvik Energiteknik AB, Nyköping
March 1987

TR 87-03

Calculations on HYDROCOIN level 1 using the GWHRT flow model

**Case 1 Transient flow of water from a
borehole penetrating a confined
aquifer**

**Case 3 Saturated-unsaturated flow
through a layered sequence of
sedimentary rocks**

**Case 4 Transient thermal convection in a
saturated medium**

Roger Thunvik, Royal Institute of Technology,
Stockholm
March 1987

TR 87-04

Calculations on HYDROCOIN level 2, case 1 using the GWHRT flow model Thermal convection and conduction around a field heat transfer experiment

Roger Thunvik
Royal Institute of Technology, Stockholm
March 1987

TR 87-05

Applications of stochastic models to solute transport in fractured rocks

Lynn W Gelhar
Massachusetts Institute of Technology
January 1987

TR 87-06

Some properties of a channeling model of fracture flow

Y W Tsang, C F Tsang, I Neretnieks
Royal Institute of Technology, Stockholm
December 1986

TR 87-07

Deep groundwater chemistry

Peter Wikberg, Karin Axelsen, Folke Fredlund
Royal Institute of Technology, Stockholm
June 1987

TR 87-08

An approach for evaluating the general and localized corrosion of carbon steel containers for nuclear waste disposal

GP March, KJ Taylor, SM Sharland, PW Tasker
Harwell Laboratory, Oxfordshire
June 1987

TR 87-09

Piping and erosion phenomena in soft clay gels

Roland Pusch, Mikael Erlström,
Lennart Börgesson
Swedish Geological Co, Lund
May 1987

TR 87-10

Outline of models of water and gas flow through smectite clay buffers

Roland Pusch, Harald Hökmark,
Lennart Börgesson
Swedish Geological Co, Lund
June 1987

TR 87-11

Modelling of crustal rock mechanics for radioactive waste storage in Fennoscandia—Problem definition

Ove Stephansson
University of Luleå
May 1987

TR 87-12

Study of groundwater colloids and their ability to transport radionuclides

Kåre Tjus* and Peter Wikberg**
*Institute for Surface Chemistry, Stockholm
**Royal Institute of Technology, Inorganic
Chemistry Stockholm
March 1987

TR 87-13

Shallow reflection seismic investigation of fracture zones in the Finnsjö area method evaluation

Trine Dahl-Jensen
Jonas Lindgren
University of Uppsala, Department of Geophysics
June 1987

TR 87-14

Combined interpretation of geophysical, geological, hydrological and radar investigations in the boreholes ST1 and ST2 at the Saltsjötunnel

Jan-Erik Andersson
Per Andersson
Seje Carlsten
Lars Falk
Olle Olsson
Allan Strähle
Swedish Geological Co, Uppsala
1987-06-30

TR 87-15

Geochemical interpretation of groundwaters from Finnsjön, Sweden

Ignasi Puigdomènech¹
Kirk Nordstrom²
¹Royal Institute of Technology, Stockholm
²U S Geological Survey, Menlo Park, California
August 23, 1987

TR 87-16

Corrosion tests on spent PWR fuel in synthetic groundwater

R S Forsyth¹ and L O Werme²
¹Studsvik Energiteknik AB, Nyköping, Sweden
²The Swedish Nuclear Fuel and Waste Management Co (SKB), Stockholm, Sweden
Stockholm, September 1987

TR 87-17

The July – September 1986 Skövde aftershock sequence

Conny Holmqvist
Rutger Wahlström
Seismological Department, Uppsala University
August 1987

TR 87-18

Calculation of gas migration in fractured rock

Roger Thunvik¹ and Carol Braester²
¹Royal Institute of Technology
Stockholm, Sweden
²Israel Institute of Technology
Haifa, Israel
September 1987

TR 87-19

Calculation of gas migration in fractured rock – a continuum approach

Carol Braester¹ and Roger Thunvik²

¹Israel Institute of Technology

Haifa, Israel

²Royal Institute of Technology

Stockholm, Sweden

September 1987

TR 87-20

Stability fields of smectites and illites as a function of temperature and chemical composition

Y Tardy, J Duplay and B Fritz

Centre de Sédimentologie et de Géochimie de la Surface (CNRS)

Institut de Géologie Université Louis Pasteur (ULP)

1 rue Blessig, F-67084 Strasbourg, France

April 1987

TR 87-21

Hydrochemical investigations in crystalline bedrock in relation to existing hydraulic conditions: Klipperås test-site, Småland, Southern Sweden

John Smellie¹

Nils-Åke Larsson¹

Peter Wikberg³

Ignasi Puigdomènech⁴

Eva-Lena Tullborg²

¹Swedish Geological Company, Uppsala

²Swedish Geological Company, Göteborg

³Royal Institute of Technology, Stockholm

⁴Studsvik Energiteknik AB, Nyköping

September 1987

TR 87-22

Radionuclide sorption on granitic drill core material

Trygve E Eriksen and Birgitta Locklund

The Royal Institute of Technology

Department of Nuclear Chemistry

Stockholm

November 1987

TR 87-23

Radionuclide co-precipitation

Jordi Bruno and Amaia Sandino

The Royal Institute of Technology

Department of Inorganic Chemistry

Stockholm

December 1987

TR 87-24

Geological maps and cross-sections of Southern Sweden

Karl-Axel Kornfält¹ and Kent Larsson²

¹SGU, Lund

²Softrock Consulting, Genarp

December 1987

TR 87-25

**The Bolmen tunnel project
Evaluation of geophysical site investigation methods**

Roy Stanfors

December 1987

TR 87-26

**The Kymmen power station
TBM tunnel
Hydrogeological mapping and analysis**

Kai Palmqvist¹ and Roy Stanfors²

¹BERGAB-Berggeologiska Undersökningar AB

²Lunds University

December 1987